

Table 1 Sectional Properties and Coefficients of Materials

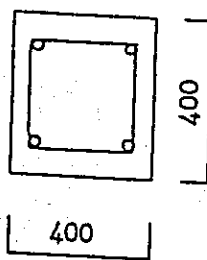
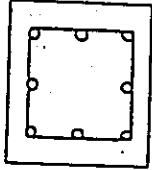
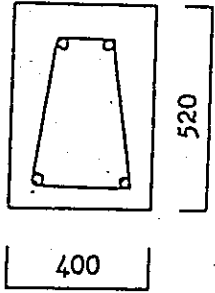
<p>Column I (4 longitudinal bars)</p>	 <p>4-32ϕ Hoop 8ϕ @50</p>	<p>Light weight concrete $E_c=1.63 \times 10^5 \text{ kg/cm}^2$ $F_c=300 \text{ kg/cm}^2$ $\gamma=1.6 \text{ ton/m}^3$ Longitudinal bar $\sigma_y=3400 \text{ kg/cm}^2$ Hoop $\sigma_y=2100 \text{ kg/cm}^2$</p>
<p>Column II (8 longitudinal bars)</p>	 <p>8-32ϕ Hoop 8ϕ @50</p>	<p>↑</p>
<p>Beam</p>	 <p>4-32ϕ Stirrup 8ϕ @60</p>	<p>↑</p>

Table 2 Weight of the Model Structure

	2F	3F	4F	5F	6F	7F	8F	9F	RF
Weight (ton)	204	204	204	204	204	204	204	204	238
Unit weight (ton/m ²)	1.05	1.05	1.05	1.05	1.05	1.05	1.05	1.05	1.22

Table 3 Equations to Calculate Properties of Beams and Columns

	Beam	Column
Cracking moment.	$M_c = 1.8\sqrt{F_c} \cdot Z \cdot \phi$	$M_c = 1.8\sqrt{F_c} \cdot Z + \frac{ND}{6}$
Yielding moment	$M_y = 0.9 a_t \cdot \sigma_y \cdot d$	$M_y = 0.8 a_t \cdot \sigma_y \cdot D + 0.5 ND \left(1 - \frac{N}{bDF_c}\right)$
Reductive Ratio of Rigidity at Yielding Point	$\alpha_y = (0.043 + 1.64n \cdot P_t + 0.043 \frac{a}{D} + 0.33\eta_0) \cdot \left(\frac{d}{D}\right)^2$	
Cracking shearing strength	$Q_c = \left\{ \frac{0.065k_c(500 + F_c)}{(M/Qd) + 1.7} \right\} b_f$	$Q_c = \left\{ \frac{\left(1 + \frac{\sigma_0}{150}\right) \cdot 0.065k_c(500 + F_c)}{(M/Qd) + 1.7} \right\} b_f$
Yielding shearing strength	$Q_u = \left\{ \frac{0.053 \cdot p_t^{0.23}(180 + F_c)}{(M/Qd) + 0.12} + 2.7\sqrt{p_w \cdot \sigma_{wy}} \right\} b_f$	$Q_u = \left\{ \frac{0.053 \cdot p_t^{0.23}(180 + F_c)}{(M/Qd) + 0.12} + 2.7\sqrt{p_w \cdot \sigma_{wy}} + 0.1\sigma_0 \right\} b_f$

F_c : Design standard strength of concrete (kg/cm²)
 Z : Section modulus. N : Axial force, D : Depth of member
 ϕ : Magnification factor for moment of inertia
 a_t : Sectional area of tensile reinforcing bar
 σ_y : Yielding strength of tensile reinforcement
 d : Depth from extreme compression fiber to the centroid of tension reinforcement in flexural member
 n : Ratio of elastic modulus of reinforcement to that of concrete, P_t : reinforcement ratio of stirrups or hoops
 b : Width of rectangular beam or column
 P_t : = a_t/bd for beam, a_t : = N/Q
 N/Q : Shear span, η_0 : = N/bDF_c , σ_0 : = N/bD
 k_c : Correction coefficient for sectional dimension
 j : Distance from the centroid of compression to the centroid of tensile reinforcement
 σ_{wy} : Yielding strength of shear reinforcement
 p_w : reinforcement ratio of stirrups or hoops

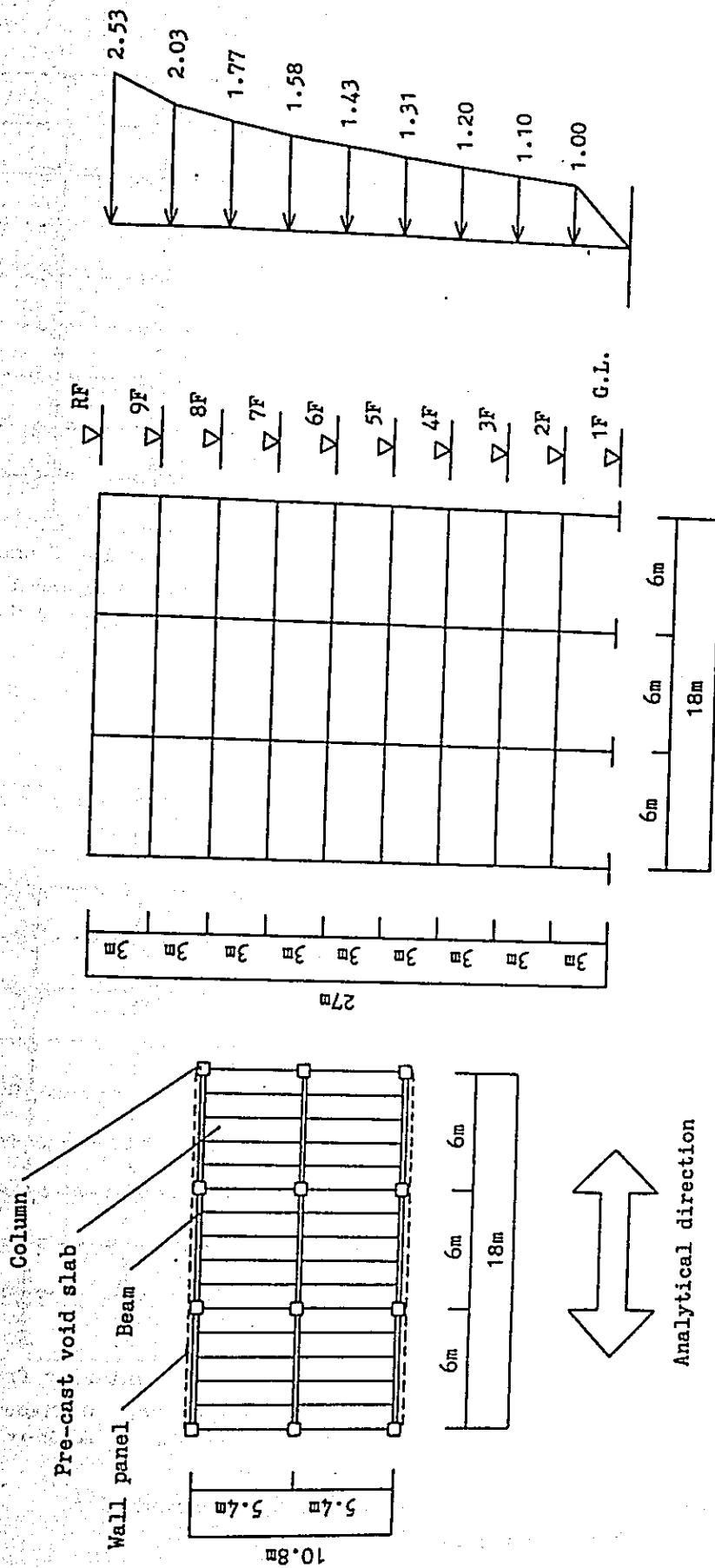


Fig. 1 Analytical Model

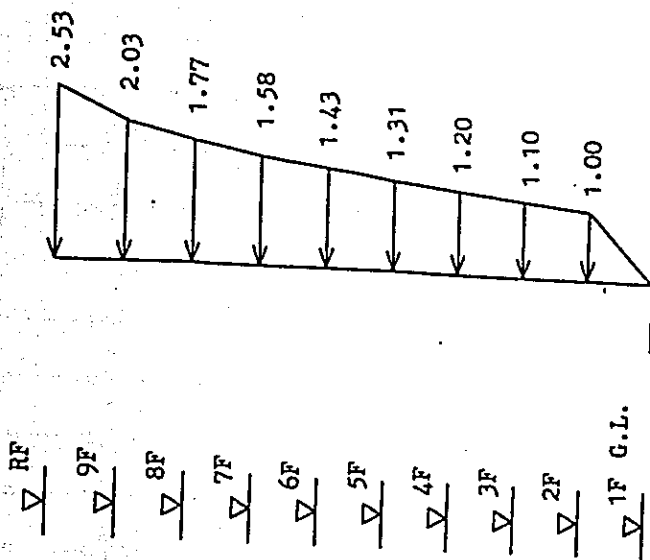
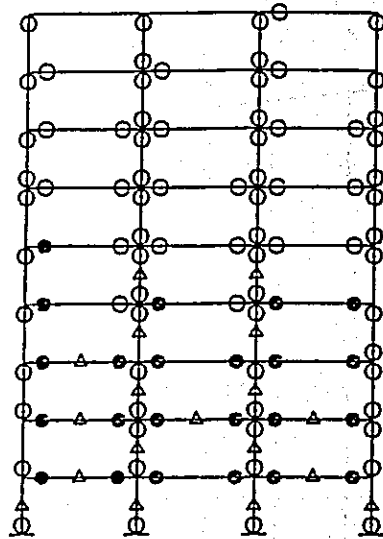


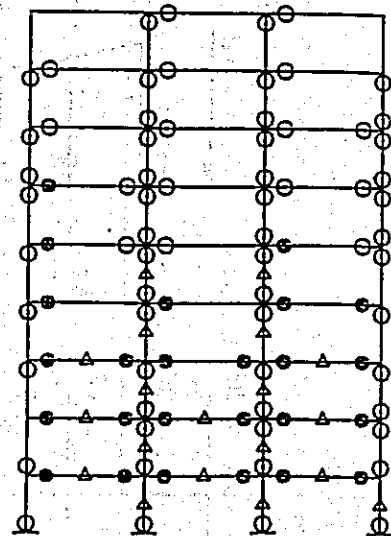
Fig. 2 Ai-distribution

Relative story displ.(cm) (angle)	Story shear (ton)
0.46 (1/650)	34.7
1.08 (1/275)	62.5
1.79 (1/170)	86.7
2.58 (1/115)	108.4
3.66 (1/80)	128.0
5.23 (1/60)	145.9
6.81 (1/45)	162.3
7.22 (1/40)	177.4
4.82 (1/60)	199.1

Displ. of top(cm)	33.7	C_B	0.102
-------------------	------	-------	-------



Exterior frame



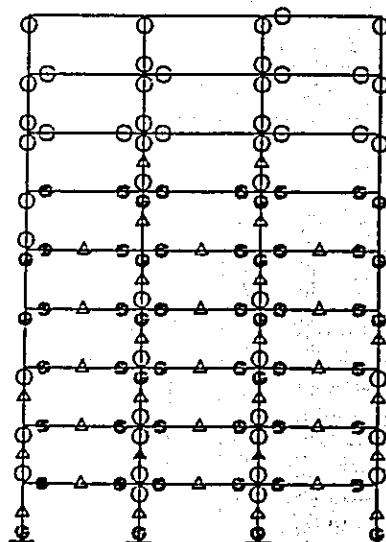
Interior frame

○: Flexural cracking ●: Flexural yielding
 △: Shear cracking ▲: Shear yielding

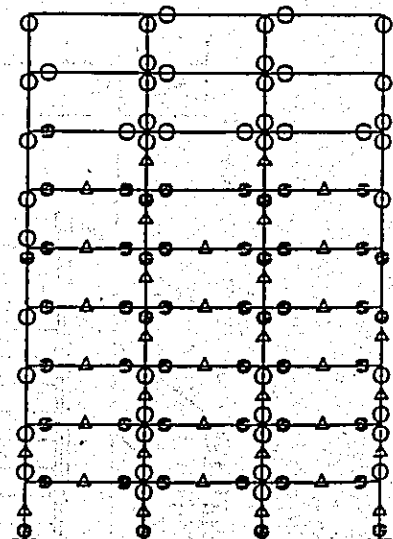
Fig.3a Plastic Hinge Formation at $C_B=0.1$
 (4 longitudinal bars)

Relative story displ.(cm) (angle)	Story shear (ton)
0.80 (1/375)	46.3
2.00 (1/150)	83.4
4.60 (1/65)	115.8
9.90 (1/30)	144.7
19.50 (1/15)	170.9
27.20 (1/11)	194.4
32.10 (1/9)	216.8
33.90 (1/9)	237.0
27.90 (1/10)	255.2

Displ. of top(cm)	159.8	C_B	0.137
-------------------	-------	-------	-------



Exterior frame



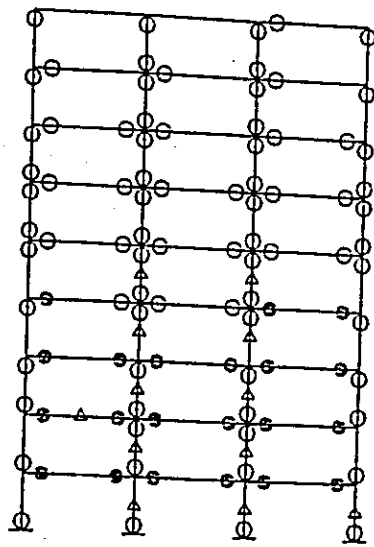
Interior frame

○: Flexural cracking ●: Flexural yielding
 △: Shear cracking ▲: Shear yielding

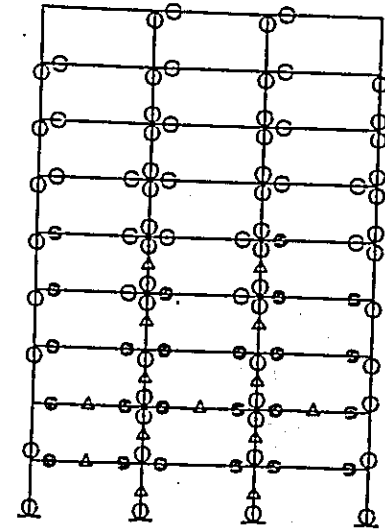
Fig.3b Plastic Hinge Formation at Collapse Mechanism
 (4 longitudinal bars)

Relative story displ. (cm) (angle)	Story shear (ton)
0.45 (1/665)	34.2
0.98 (1/305)	61.6
1.59 (1/190)	85.4
2.24 (1/135)	106.8
3.08 (1/95)	126.1
4.25 (1/70)	143.8
5.46 (1/55)	160.0
5.75 (1/50)	174.8
3.73 (1/80)	188.3

Displ. of top(cm)	27.5	C_B	0.101
-------------------	------	-------	-------



Exterior frame



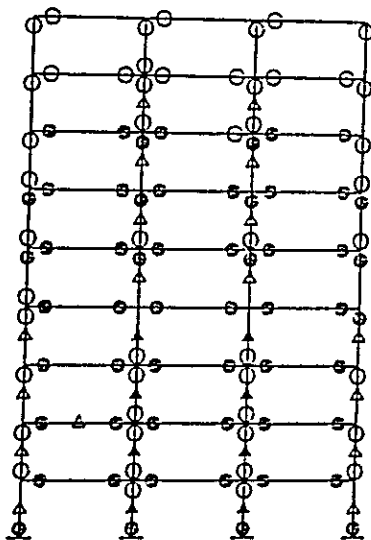
Interior frame

○: Flexural cracking ●: Flexural yielding
 △: Shear cracking ▲: Shear yielding

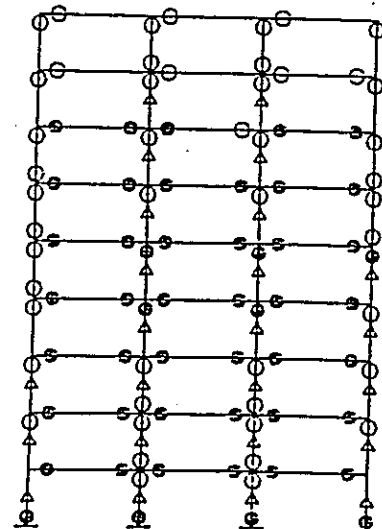
Fig.4a Plastic Hinge Formation at $C_D=0.1$
 (8 longitudinal bars)

Relative story displ. (cm) (angle)	Story shear (ton)
1.00 (1/300)	51.4
3.00 (1/100)	92.6
7.60 (1/40)	128.5
15.90 (1/19)	160.6
26.00 (1/12)	189.6
33.70 (1/9)	216.2
39.10 (1/8)	240.5
40.60 (1/7)	262.8
35.10 (1/9)	283.1

Displ. of top(cm)	202.1	C_B	0.151
-------------------	-------	-------	-------



Exterior frame



Interior frame

○: Flexural cracking ●: Flexural yielding
 △: Shear cracking ▲: Shear yielding

Fig.4b Plastic Hinge Formation at Collapse Mechanism
 (8 longitudinal bars)

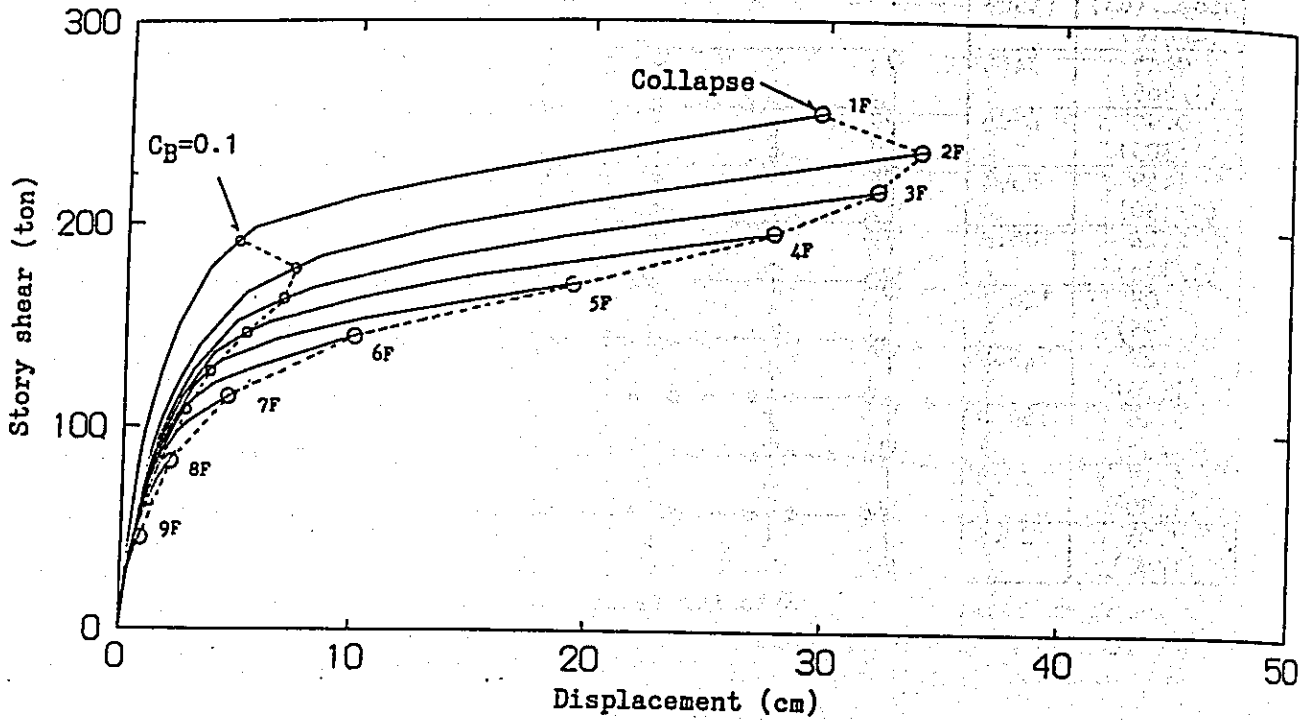


Fig.5a Relationship between Relative Story Displacement and Story Shear (4 longitudinal bars)

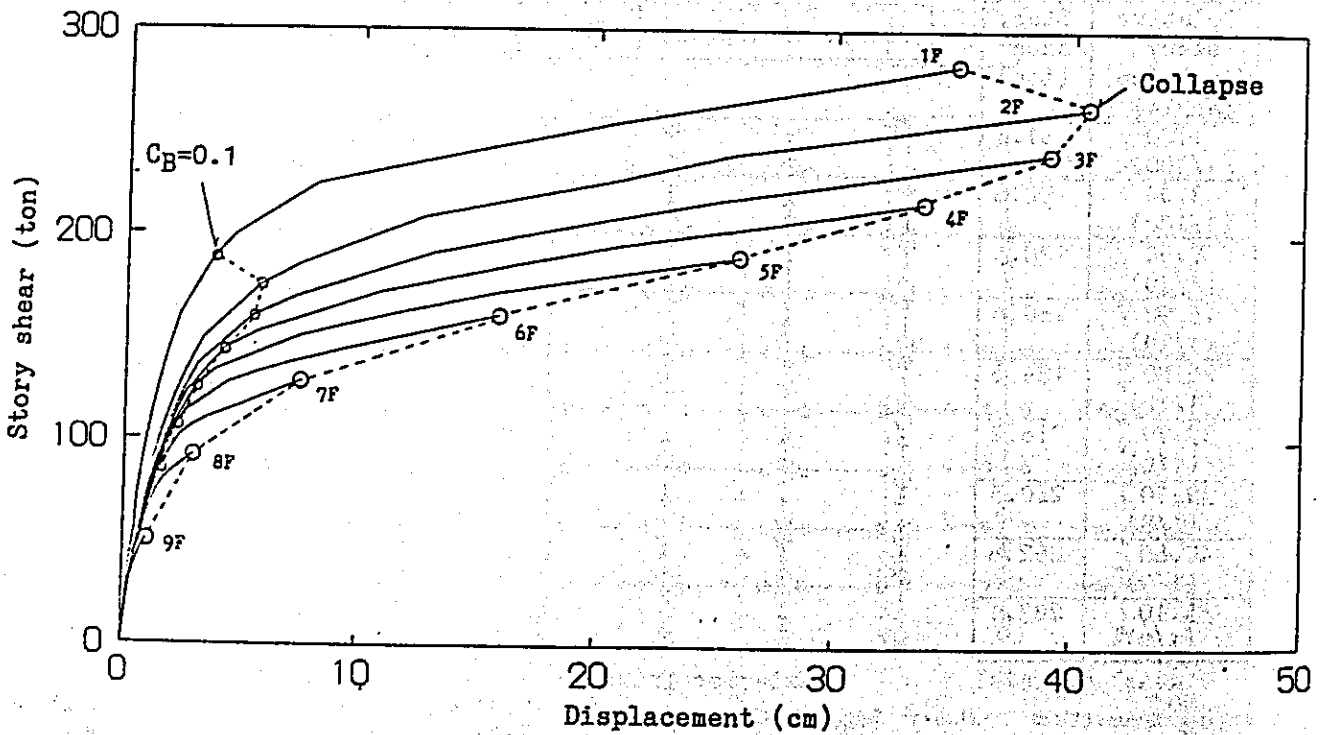
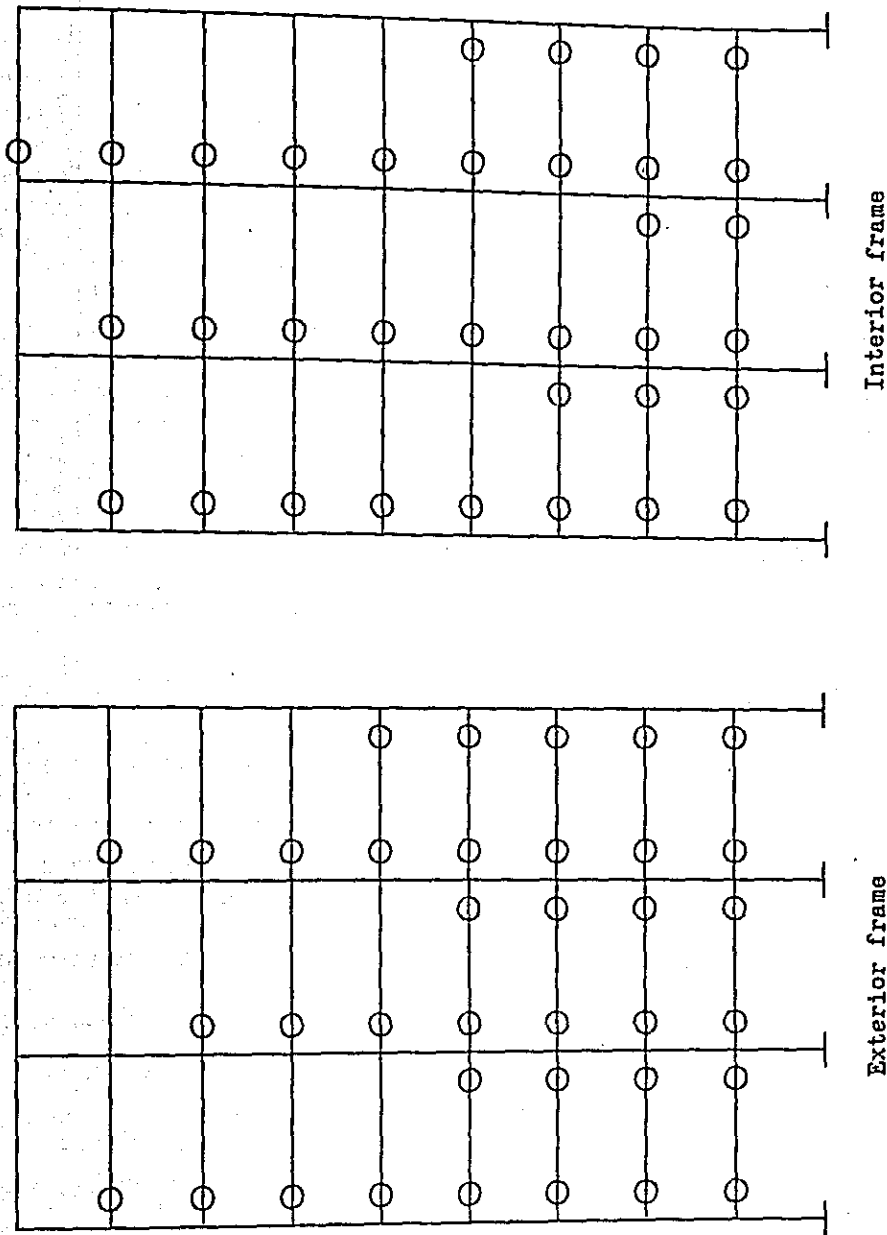


Fig.5b Relationship between Relative Story Displacement and Story Shear (8 longitudinal bars)

Maximum story displ. (cm) (angle)	Maximum Story shear (ton)
0.27 (1/1150)	24.7
0.47 (1/640)	40.1
0.63 (1/450)	50.0
0.80 (1/380)	58.7
1.12 (1/270)	75.3
1.50 (1/200)	90.8
1.79 (1/170)	103.7
1.81 (1/165)	109.7
1.28 (1/235)	113.8

Max. displ. of top(cm)	9.01	Max. C_B	0.061
------------------------	------	------------	-------



○: Flexural cracking ●: Flexural yielding
 △: Shear cracking ▲: Shear yielding

Fig.6 Plastic Hinge Formation (Main Shock at Gukaslan)

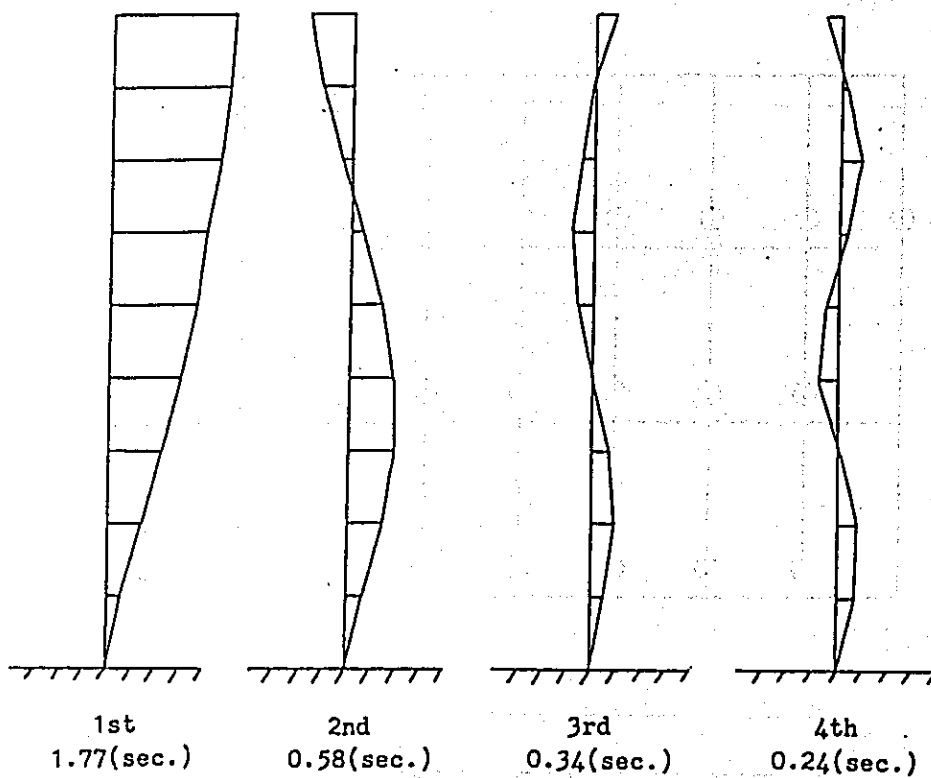


Fig.7 Natural Periods and Vibration Modes

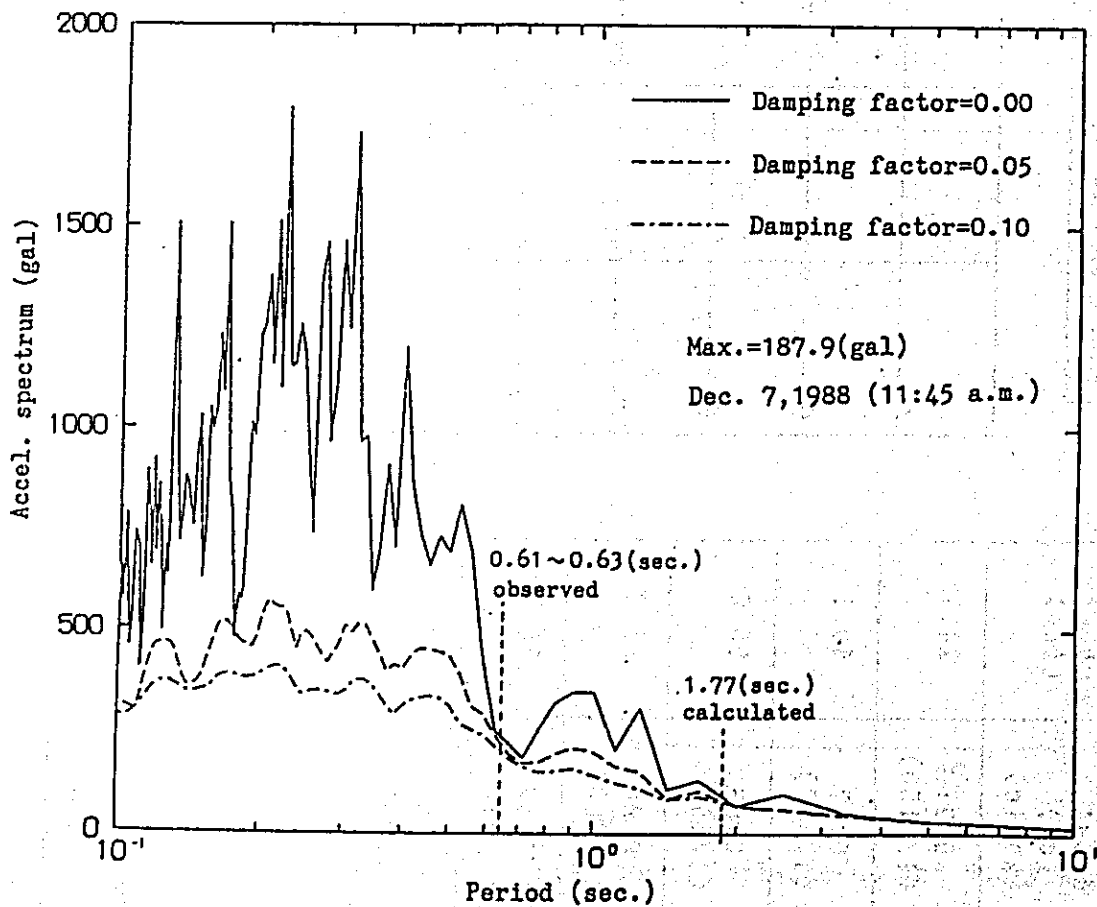


Fig.8 Acceleration Response Spectrum (Main Shock at Gukasian)

5. Dynamic Properties of Ground and Buildings in Armenia Based on Measurement of Microtremors

5.1 Abstract

The dynamic properties of surface ground are well known to effect the damage degree of buildings during the earthquake. And also, the shapes of Fourier spectrum of microtremors are well known to similar to the shapes of Fourier spectrum of strong motion earthquakes. This paper describe the relation between the dynamic properties of ground based on the measurement of microtremors and the damage degree of the buildings.

5.2 General Characteristics of Microtremors

Definition of Microtremors Microtremor is defined as ground vibration by artificial sources which are caused by traffics or machineries in the city area, and it is differ from microseism that is caused by natural meteological phenomena. The amplitude of microtremor is smaller than 10 micrometer and the range of period is 0.5 to 2 or 3 seconds, (some times 4 to 5 seconds). The amplitude of microtremor is changed according to the time, that is, day-time is 3 times larger than night-time.

Relation between Layered Structure of Surface Soil and Predominant Period of Fourier Spectrum of Microtremors In the layered soil structure, seismic waves propagate with multiple reflection. And as the results of multiple reflection, it has own period. This own period is appeared as the predominant period of microtremors.

Relative Assessment of the Amplitude of Fourier Spectrum of Microtremors The shape of Fourier spectrum of microtremors is similar to the shape of Fourier spectrum of strong motion earthquakes. The amplitude of Fourier spectrum of strong motion earthquake is equivalent to the amplitude of Fourier spectrum of microtremors.

5.3 Results of Dynamic Properties of Buildings in Armenia

Microtremors Measured on Buildings The microtremors on the buildings were measured 19 sites in Yerevan, Leninakan and Kirovakan. The measurement in Yerevan were recognized for the dynamic properties of un-damaged buildings. The measurements in Leninakan and Kirovakan were recognized for the properties of damaged buildings. The measurement results are shown in Table 1. In this Table, the natural period and critical damping coefficient of translation and torsional modes for the longitudinal and transverse directions of each building.

Comparison of Dynamic Properties Between Un-Damaged and Damaged Buildings

1) 5-story Stone-Masonry Building: The natural periods and critical damping coefficients of un-damaged buildings are 0.28 - 0.33 sec. and 2.2 - 7.2 %.

*1 Professor Emeritus, Tokyo Institute of Technology

*2 Head, Earthquake Engineering Laboratory, National Research Center for Disaster Prevention, Science and Technology Agency

respectively. The natural periods and critical damping coefficients of damaged buildings are 0.21 - 0.55 sec., 1.9 - 4.4 %, respectively. The difference of the natural periods of damaged buildings are so large, because it is guessed that this causes is based upon the deteriorative effects of walls.

2) 9-story Precast Reinforced Concrete Frame Building: The natural periods of un-damaged buildings in the longitudinal direction and transverse direction are 0.61 - 0.63 sec. and 0.46 - 0.53 sec., respectively. The natural periods of damaged buildings in the longitudinal and transverse directions are 0.83 - 1.07 sec., 0.81 - 1.00 sec., respectively. The natural periods of damaged buildings are increased about 30 - 40 % compared with the periods of un damaged buildings. The critical damping coefficients of damaged buildings are 25 % larger than those of un damaged buildings.

3) 9-story Large-Size Panel Building: The natural periods and critical damping coefficients of un-damaged buildings are 0.38 - 0.39 sec. and 1.2 - 2.5 %, respectively. The natural periods and critical damping coefficients of damaged buildings are 0.40 - 0.46 sec. and 2.6 - 4.5 %, respectively. The natural periods are not so changed between un-damaged and damaged buildings, but the critical damping coefficients of damaged buildings are almost 2 times those of un-damaged buildings.

5.4 Measurements of Microtremor on Ground

The measurements of microtremor on the ground surface are done for the grasping of the dynamic properties of ground. The measurements were made to the following two objectives:

1) The damaged buildings have the natural periods of around 0.5 sec. of precast reinforced concrete frame building in Leninakan and the natural periods of around 0.3 sec. of stone-masonry building in Spitak and Kirovakan. Therefore, the microtremors were measured by the short period seismometer (the natural period of pendulum is 1 second).

2) The microtremors by the long period seismometer (the natural period of pendulum is 3 second) were measured for the estimation of deeper ground structures in Leninakan.

5.5 Microtremors Measured in and around Leninakan

The microtremors of ground were measured at 12 points in and around Leninakan. The measured points are shown in Fig. 1. The wave forms of microtremors are shown in Fig. 2. Fig. 2-(a) shows the six points (11, 1, 3, 6, 9, 10) which are lined from north to south direction of Leninakan city. Figs. 2-(b), 2-(c) and 2-(d) show the 5 points (11, 12, 4, 7, 10) from north to south of different line of Fig. 2-(a), 4 points (2, 1, 12, 5) and 3 points (6, 7, 8) from west to east, respectively. Fig. 2-(e) shows the 3 points of New Leninakan sites by the measuring of long period seismometer. The Fourier spectrum of each point are shown in Figs. 3-(a) to 3-(c).

Seismic Bedrock of Leninakan The microtremors by long period seismometer in the new developing area of northern Leninakan find the predominant period of 3 - 4 sec. This long predominant period is caused by the very deep sedimentary layer on the seismic bedrock. This fact shows that the seismic bedrock of Leninakan area will be located at the several kilometers bellow the ground surface. The long predominant period in the new developing area of southern Leninakan is close to the period in the northern part area. Therefore, the seismic bedrock in and around Leninakan area is located at almost same depth.

Relation between Mean Period of Microtremors and Degree of Building Damage

- 1) In the northern area of Leninakan (north part from Lenin square): The mean period of microtremors of ground is about 0.5 sec., and this period is close to the natural period of 9-story precast reinforced concrete frame buildings. So it is guessed that this fact might be one of cause of making damages of this kind of buildings more seriously.
- 2) In the central area of the city: The mean period of microtremors of ground is 0.2 - 0.3 sec., and this period is close to the natural period of low-rise stone masonry buildings. This fact might be one of cause of making damages of this kind of buildings more seriously. It is necessary to implement the more detailed survey, because there are under ground flows of Kymairi river.
- 3) In the southern area of Leninakan: The mean period is close to the period in the northern area, but it's amplitude is larger than of the northern area.
- 4) General trend of dynamic properties of ground in and around Leninakan: Leninakan city is located on the deep sedimentary layer, and the predominant periods of microtremors are effected by the local sedimental condition of surface layer. And so, the amplitude of microtremors of some areas have remarkably large according to the material of surface ground at the very shallow part. These facts might be caused the degree of damages of buildings.

5.6 Microtremors Measured in and around Spitak

The microtremors of ground were measured at 10 points in and around Spitak. The measured points are shown in Fig. 4. The wave forms of microtremors of each points are shown in Fig. 5, and the Fourier spectrum are shown in Fig. 6-(a) to 6-(c).

Seismic Bedrock of Spitak The predominant period is very short (less than 0.1 sec.) at the foot around the hill, where a monument was constructed at the top of this hill. The seismic bedrock is located at the very shallow in these area. Therefore, the dynamic properties does not appeared in the microtremor, and the amplitude during the earthquake was comparatively small.

Relation between Mean Period of Microtremors and Degree of Building Damages The predominant periods in heavy damaged area of Spitak are the range between 0.2 sec. and 0.4 sec., and these periods are close to the natural period of destroyed buildings. So it is guessed that this fact might be one of causes of making damages of this kind of buildings more seriously. And then, the other cause of making damages is very strong earthquake motion itself.

New Developing Area of Spitak The predominant period in new developing area of Spitak is almost close to that in the damaged area of Spitak. Therefore, it is necessary to construct the more reinforced and more stiffened buildings.

5.7 Microtremors Measured in and around Kirovakan

The microtremors of ground were measured at 5 points in and around Kirovakan. The measured points are shown in Fig. 7. The wave forms and the Fourier spectrum of microtremor at each point are shown in Fig. 8 and Fig.9-(a) to Fig. 9-(b), respectively.

Relation between Mean Period of Microtremors and Degree of Building Damages The amplitude of microtremor at the just front of the City-Office (point 2) is about 1/3 times of the amplitude in heavy damaged area. The predominant period in heavy damaged area, where is located very close to the City-Office, is 0.2 - 0.4 sec. This fact might be one of the causes of making damages of building

more seriously.

New Developing Area of Kirovakan The predominant period in new developing area of Kirovakan is a little longer than the period in the damaged area of Kirovakan.

5.8 Relation between the Ground Properties at the Narrow Valley and the Earthquake Damages

At the city area, which is located at the comparatively narrow valley in the mountain zone (for example, the area of Spitak or Kirovakan), the relations between the ground properties and the earthquake damages will be appointed generally as follows;

- 1) At the area of the outcrop part of seismic bedrock or on the very shallow sedimentary layer, the damages of buildings were not so severe. And, the amplitude of microtremors is small at the range of short periods, but is relatively large at the range of longer periods. (example: the hill area of Spitak, point 7. the central part of Kirovakan, point 2)
- 2) The building damages were more severe by the more thickness of the sedimentary layer. But, it is very clear to find the relation between the damage and the selectivity of predominant period. The amplitude of microtremors is remarkably large at the range of short period, but is not so remarkable at the range of longer period. (example: the housing complex area of northern part of Spitak, point 2. the housing complex area of north-western part of Leninakan, point 1)

5.9 Relation between the Earthquake Damages and the Seismic Microzoning

The one of causes of heavy damage of buildings is able to explain the coincidence between the predominant period of ground and the natural period of building. The other cause is very strong earthquake motion itself. Therefore, it is necessary to more consideration of dynamic properties of ground for the Seismic Microzoning. The measurements of microtremors on ground and building are very effective procedure to estimate the predominant period of ground and the natural period of building.

5.10 Acknowledgement

Measuring of the microtremors were carried out by the apparatus of Tokyo Institute of Technology and great cooperations on the digitization and analysis were obtained from Dr. Kazuoh SEO, Associated Professor and Mr. Takanori SAMANO, Assistant, Tokyo Institute of Technology. The cooperations are deeply acknowledged.

Table 1 Dynamic Properties of Damaged and Un-damaged Buildings

Type of Structure and No. of Story	Damage #1	Translation				Torsional			
		Longitudinal		Transverse		Longitudinal		Transverse	
		T sec	h %	T sec	h %	T sec	h %	T sec	h %
Stone Masonry 5	U	0.30	4.8	0.33	7.2	0.35	2.6	0.35	4.6
	U	0.28	2.2	0.28	4.6	0.23	1.8	0.23	1.1
	D	0.49	4.0	0.28	1.9	0.41	4.7	0.41	3.6
	D	0.44	2.6	0.21	1.9	0.40	3.6	0.40	4.5
	D	0.52	4.0	0.52	7.4	0.55	3.2	0.56	4.1
	D	0.55	3.4	0.55	4.4	0.56	5.9	0.59	4.7
Precast Frames 9	U.U	0.57	1.6	0.79	1.1	0.50	9.3	0.54	15.0
	U.U	0.43	11.1	0.63	1.4	0.41	9.9	0.41	4.7
	U	0.61	3.2	0.46	1.7	0.41	0.6	0.42	2.5
	U	0.63	0.5	0.53	2.3	0.55	3.4	0.55	3.4
	D	0.93	---	0.93	---	0.87	---	0.85	---
	D	1.07	---	0.96	---	0.95	---	0.95	---
	D	1.00	---	0.81	---	0.80	---	0.77	---
	D	0.83	---	1.00	---	0.77	---	0.78	---
Large Pnel 9	U	0.38	2.2	0.38	1.2	0.30	2.3	0.30	0.5
	U	0.38	1.8	0.39	2.5	0.29	1.4	0.29	0.5
	U	0.46	4.5	0.40	2.6	0.46	3.4	0.45	1.8
Monolithic 4	U	0.51	2.6	0.32	2.2	0.27	0.9	0.27	2.9
Monolithic 16	U	1.10	7.8	1.00	6.1	0.96	1.9	1.18	1.3

--- unknown #1 U:Undamaged D:Damaged U. U:Undamaged and Under Construction

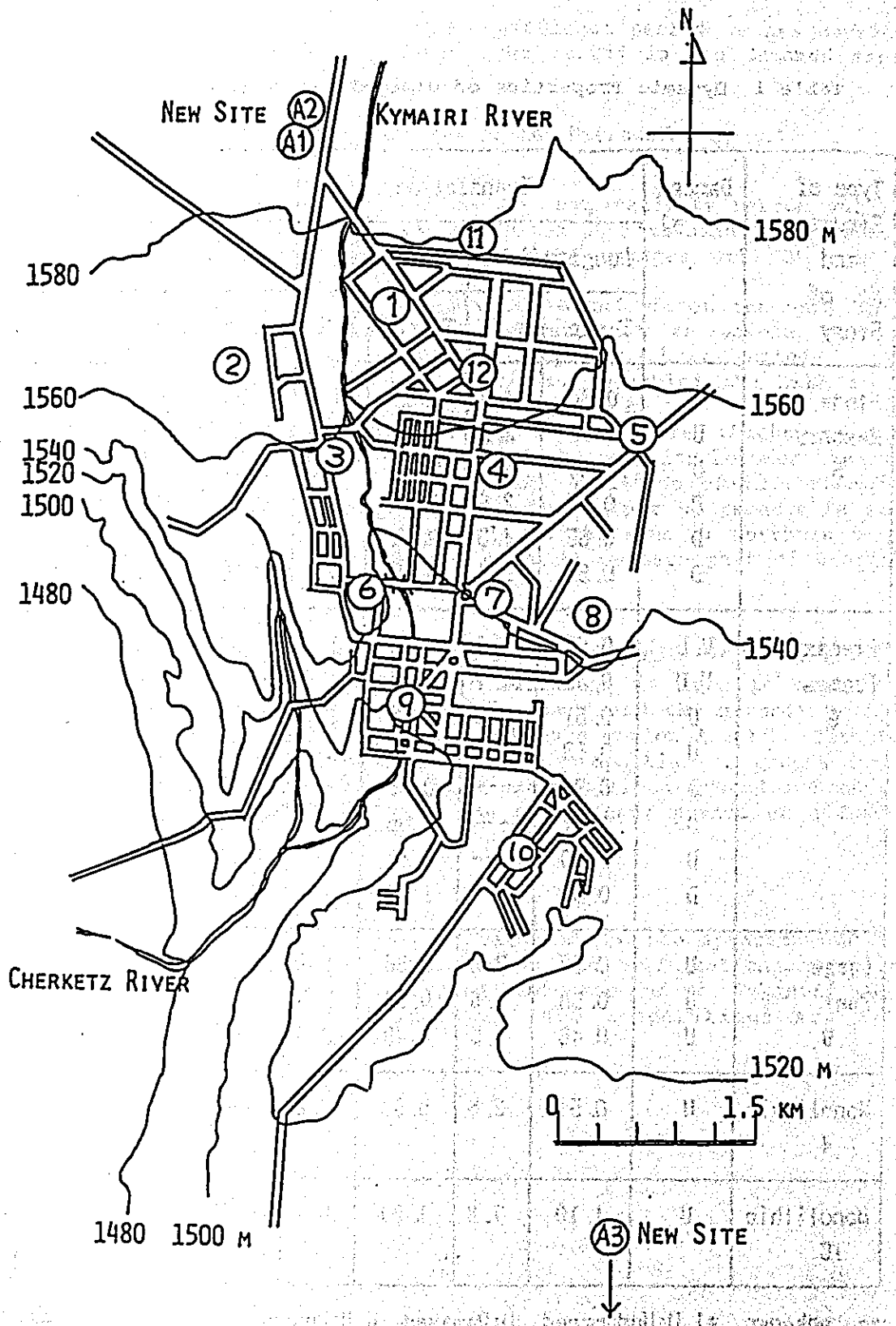


Fig. 1 Measured Points of Microtremors in LENINAKAN

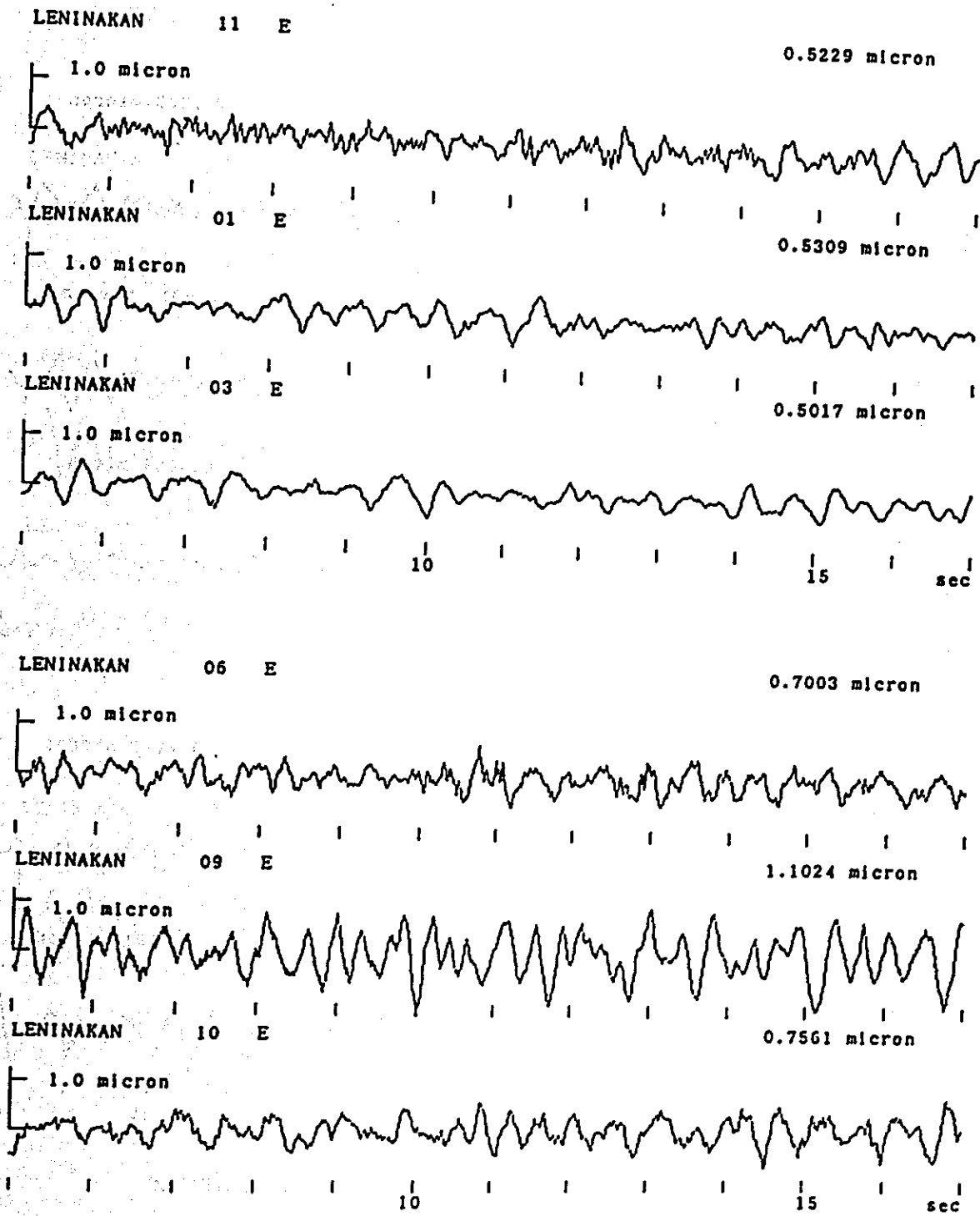


Fig. 2-(a) Wave Forms of Microtremors in LENINAKAN

LENINAKAN 11 E

0.5229 micron

1.0 micron

LENINAKAN 12 E

0.6017 micron

1.0 micron

LENINAKAN 04 E

0.4907 micron

1.0 micron

10

15

sec

LENINAKAN 07 E

0.5211 micron

1.0 micron

LENINAKAN 10 E

0.7561 micron

1.0 micron

10

15

sec

Fig. 2-(b) Wave Forms of Microtremors in LENINAKAN

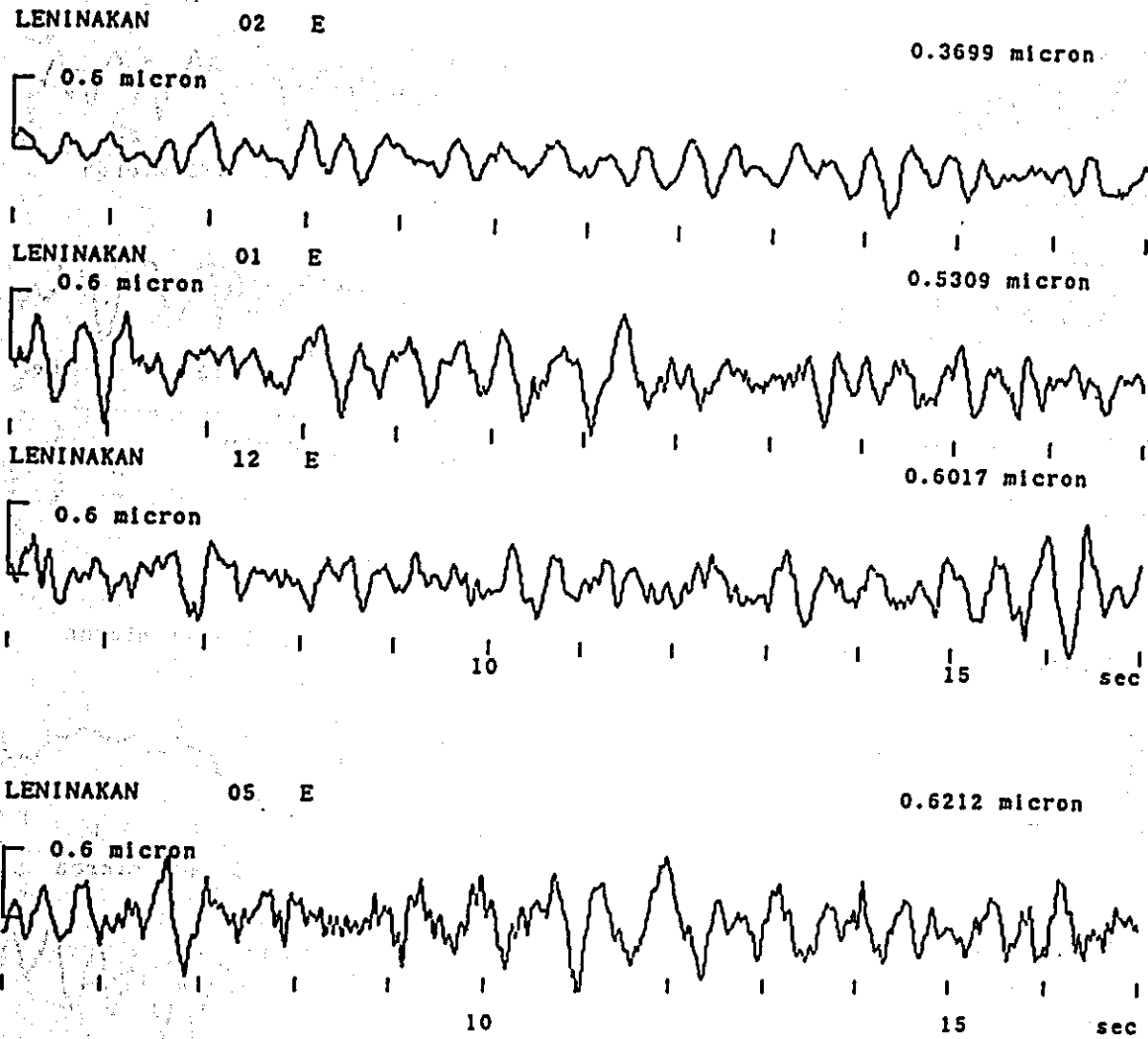


Fig. 2-(c) Wave Forms of Microtremors in LENINAKAN

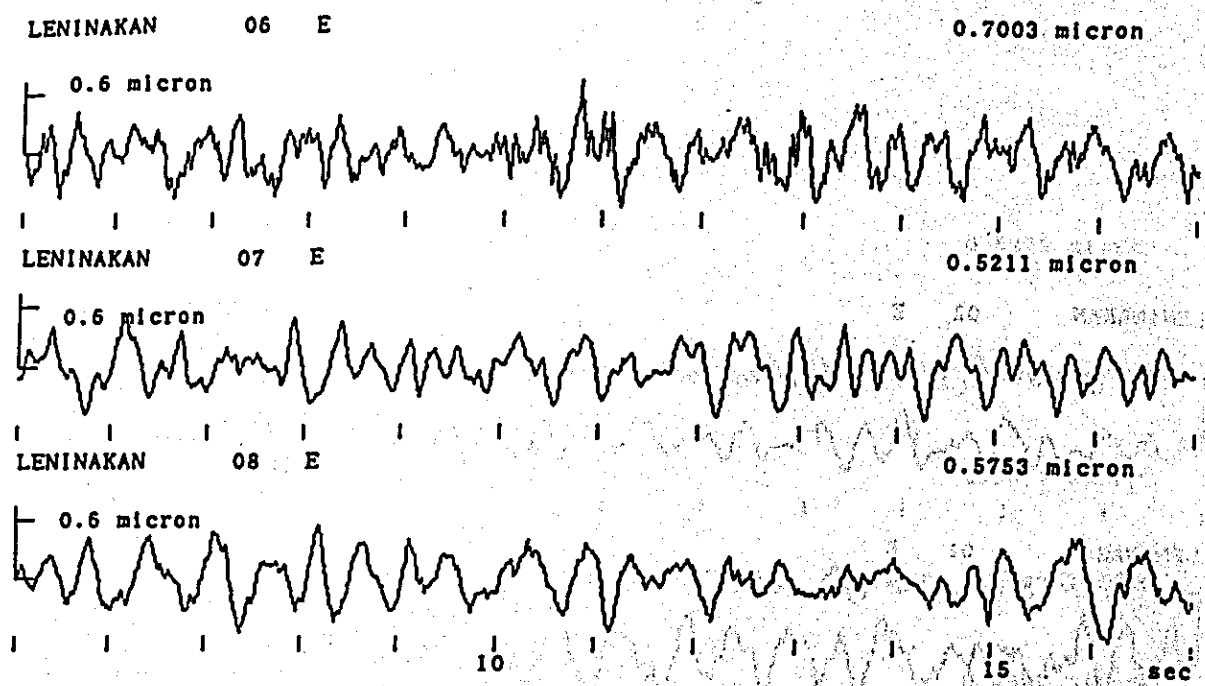


Fig. 2-(d) Wave Forms of Microtremors in LENINAKAN

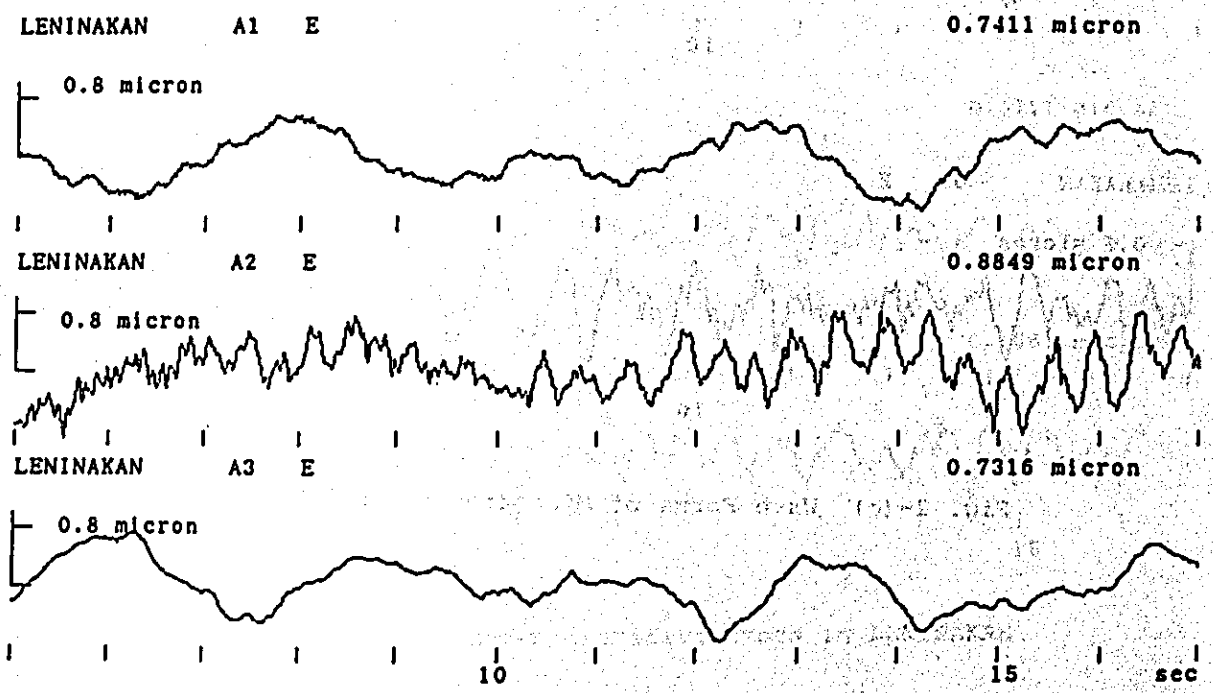


Fig. 2-(e) Wave Forms of Microtremors in LENINAKAN
(by Long Period Seismometer)

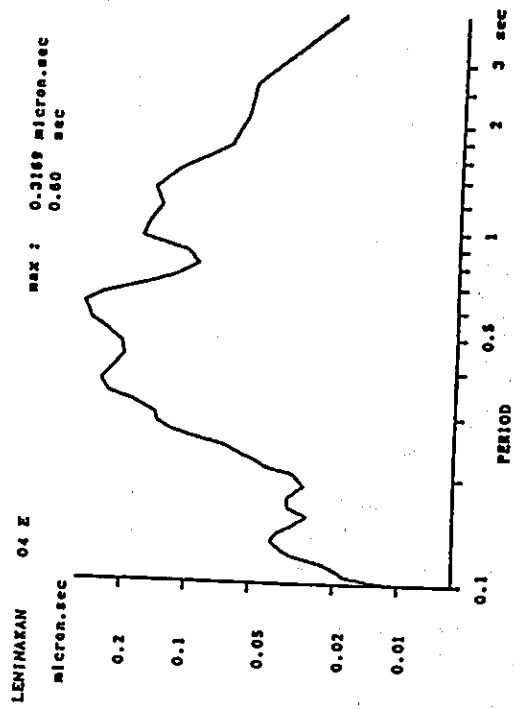
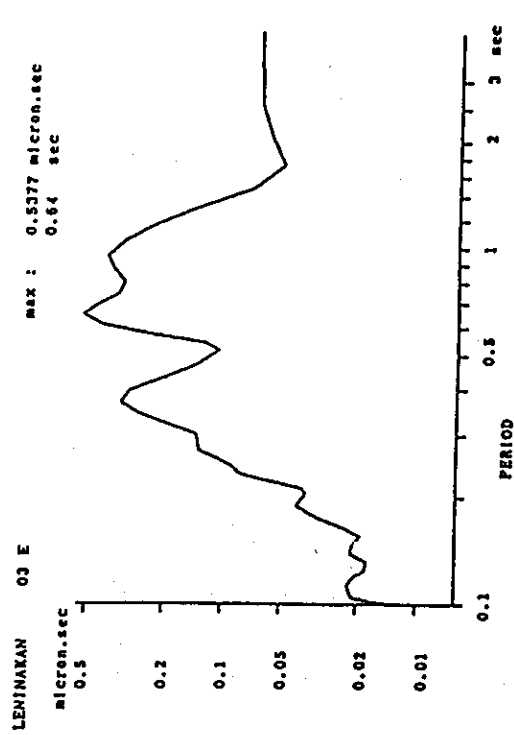
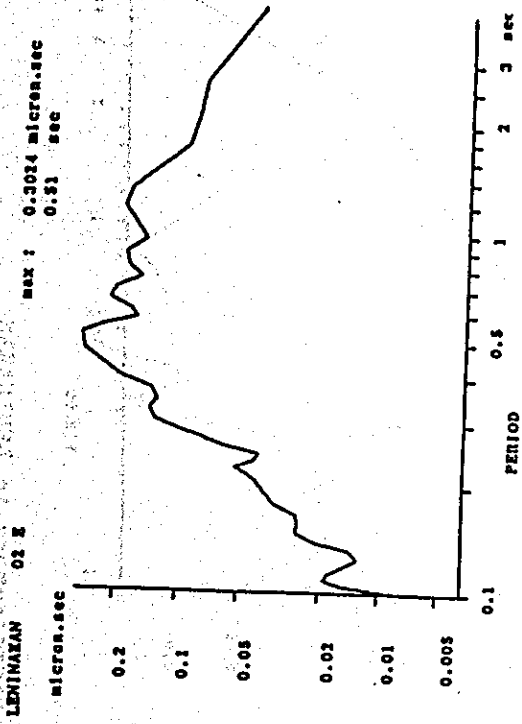
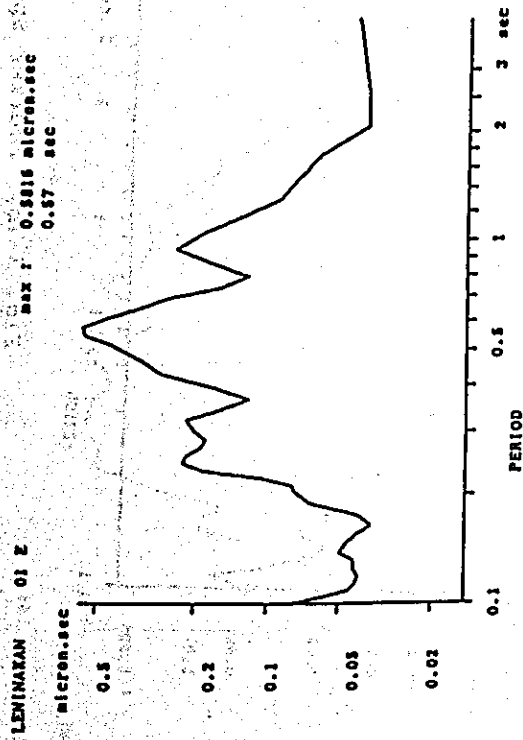


Fig. 3-(a) Fourier Spectra of Microtremors in LENINAKAN

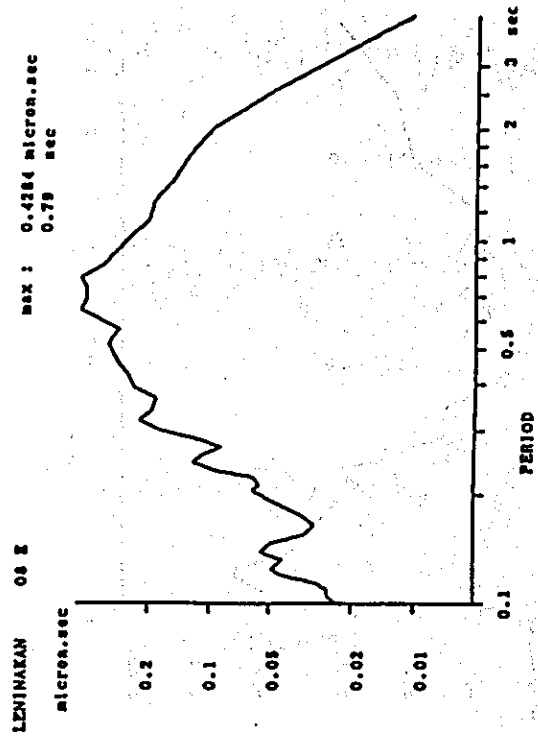
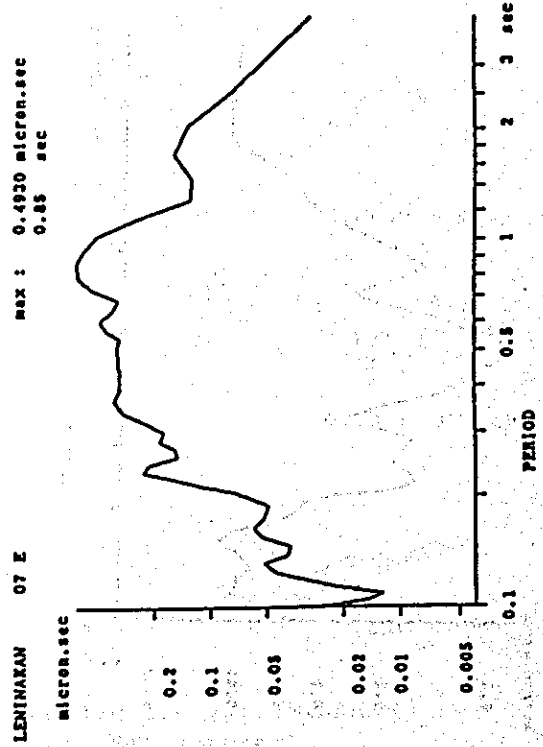
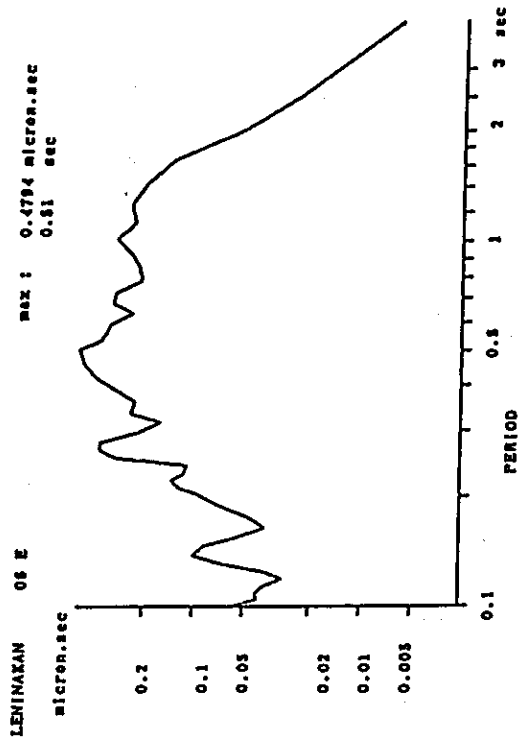
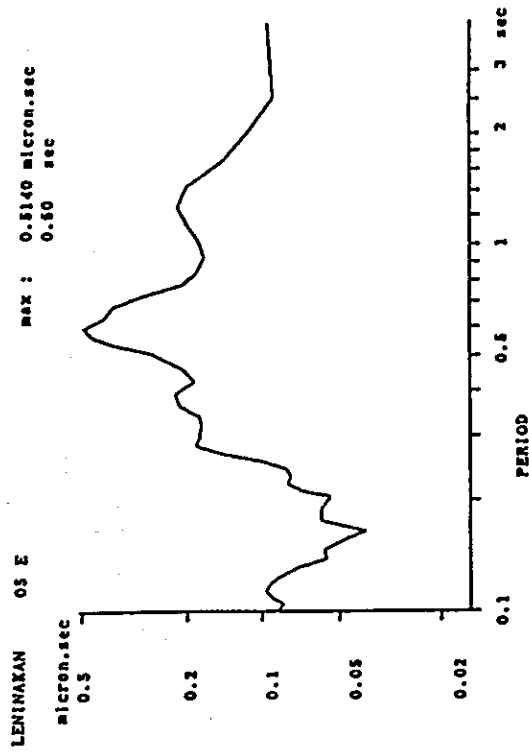


Fig. 3-(b) Fourier Spectra of Microtremors in LENINAKAN

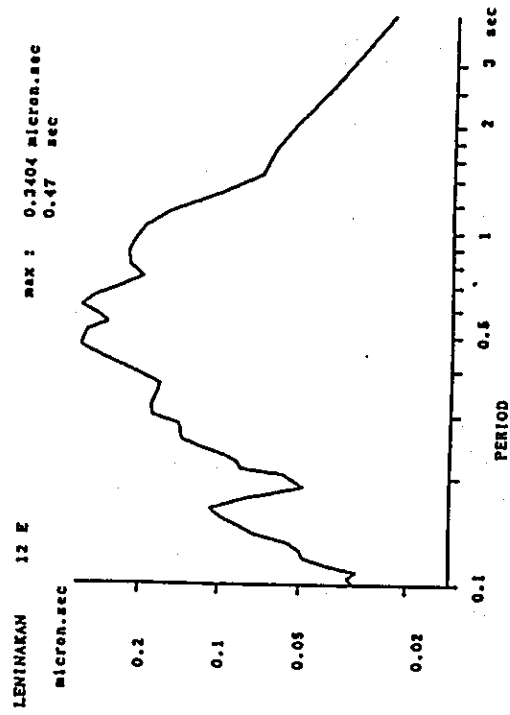
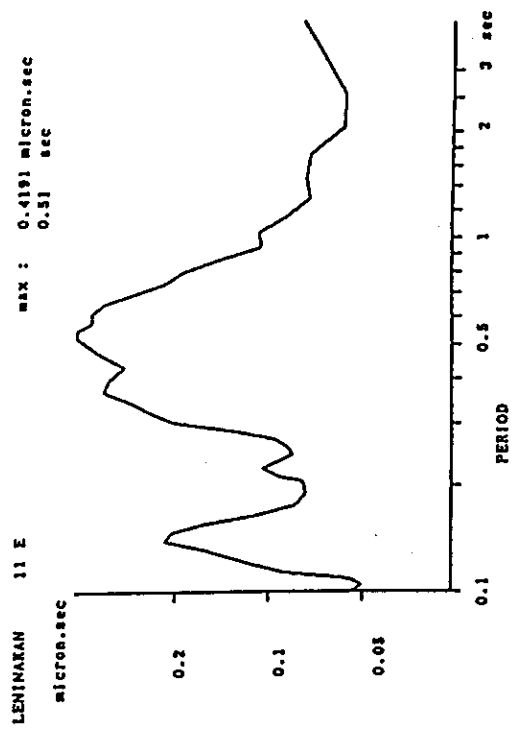
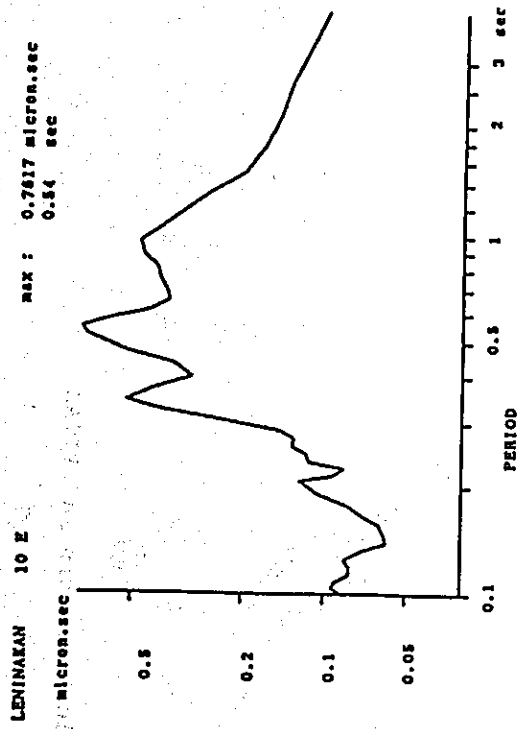
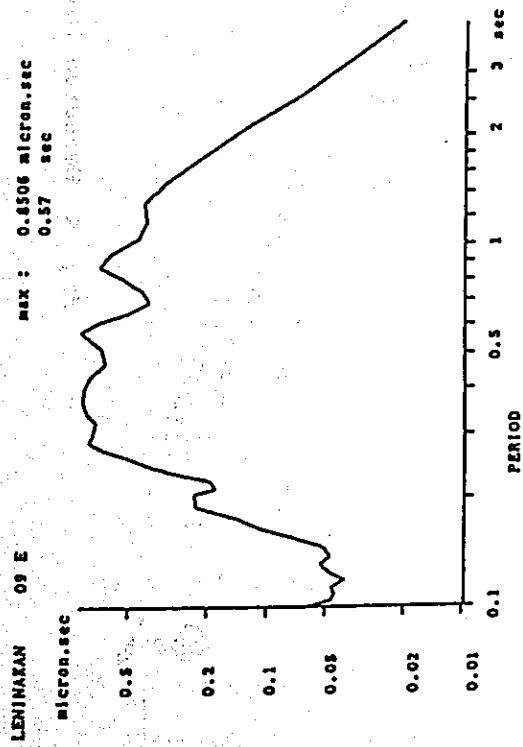


Fig. 3-(c) Fourier Spectra of Microtremors in LENINAKAN

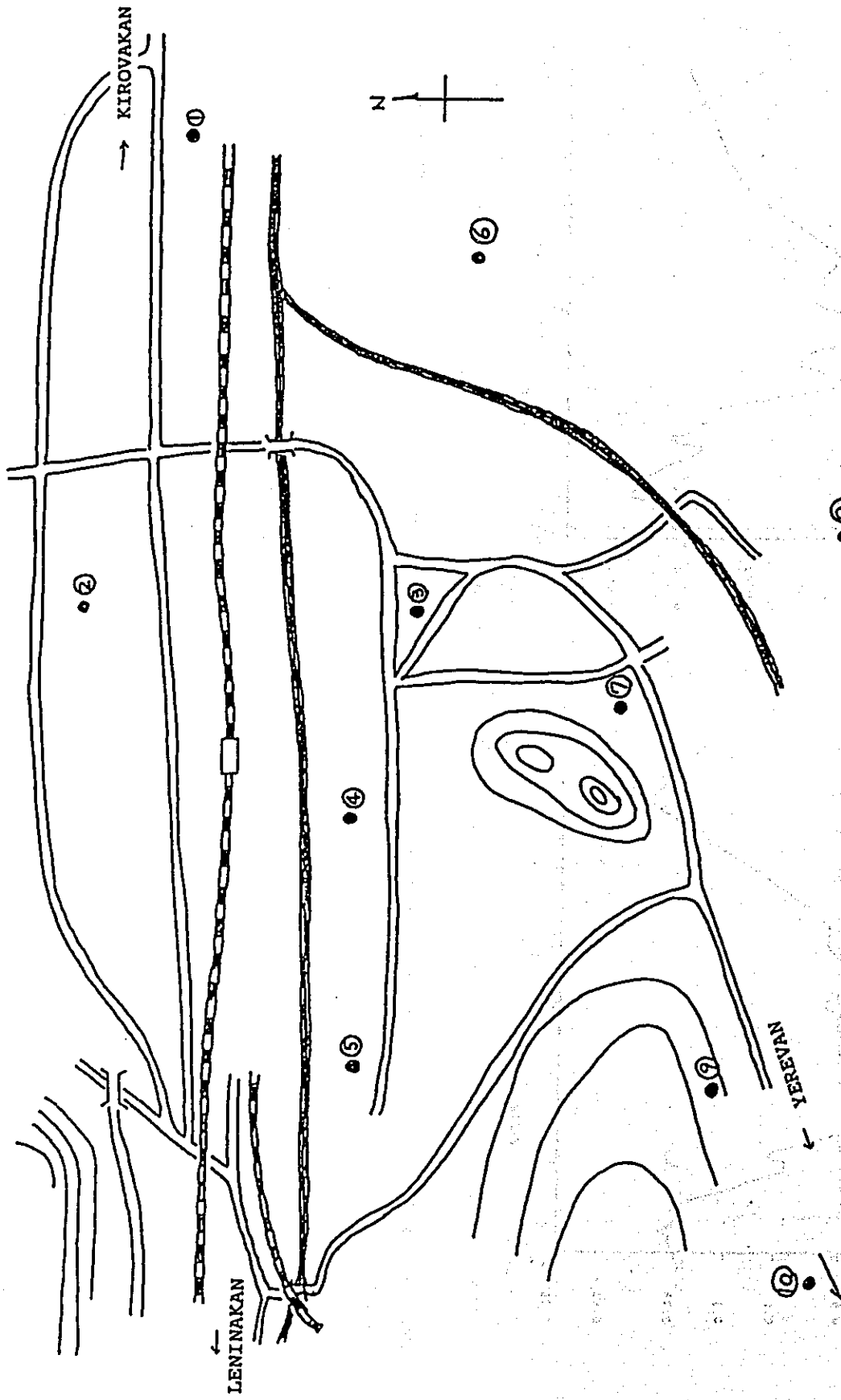


Fig. 4 Measured Points of Microtremors in SPITAK

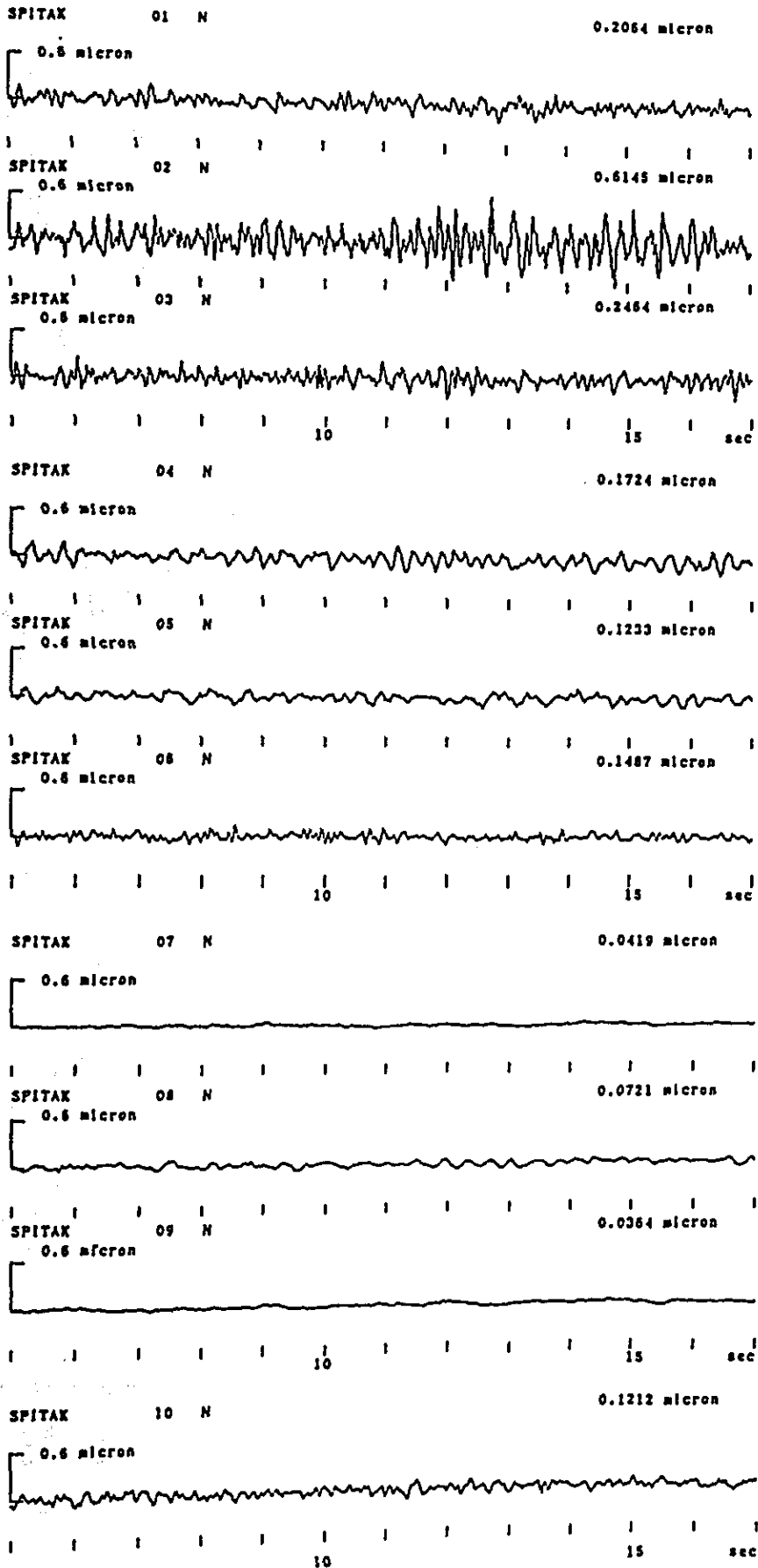


Fig. 5 Wave Formes of Microtremors in SPITAK

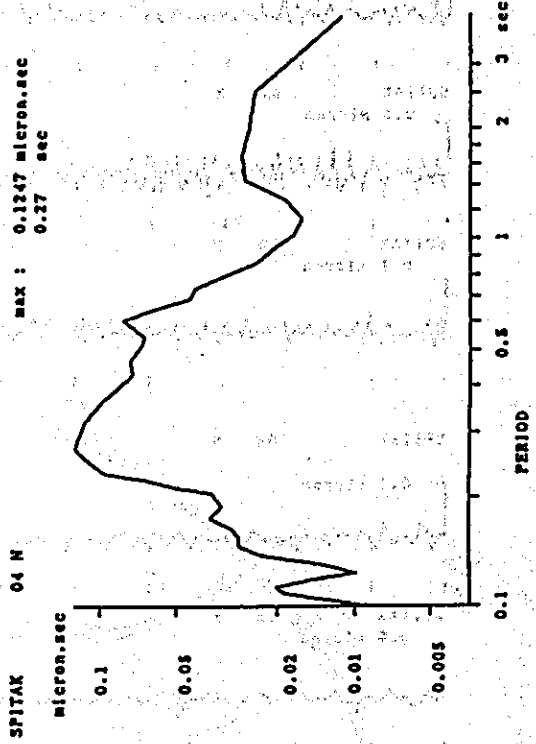
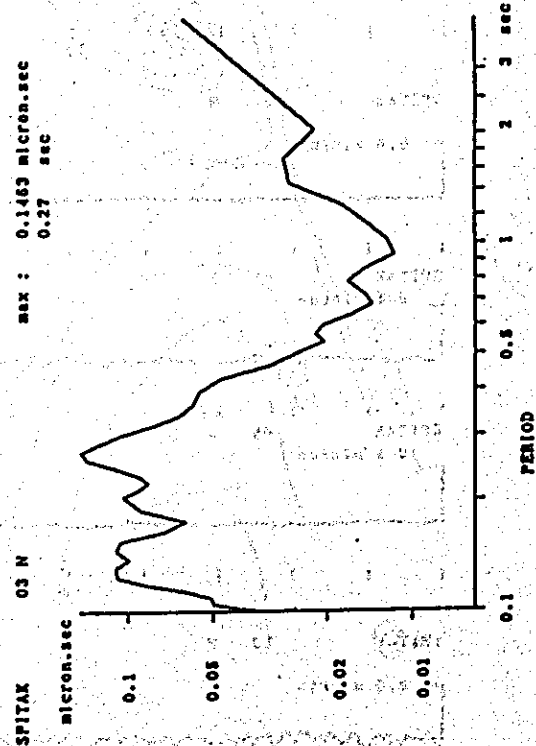
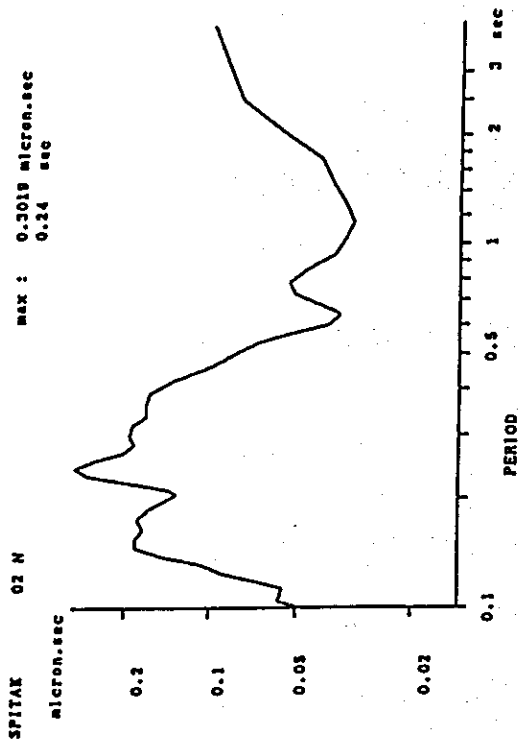
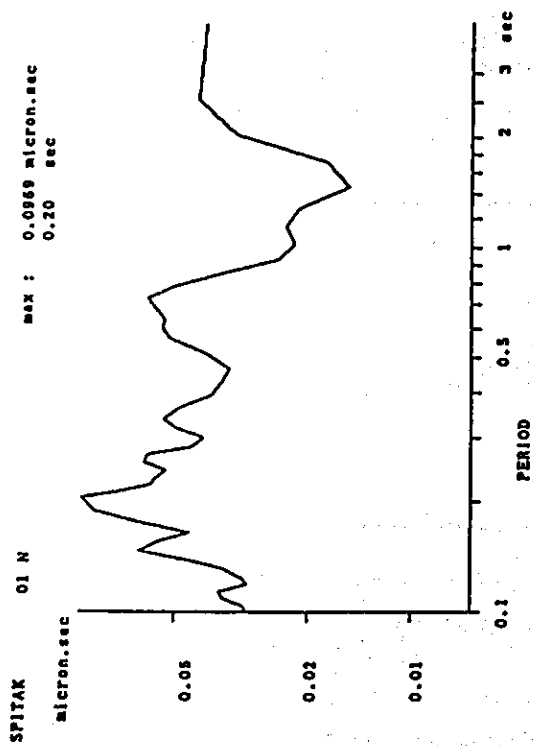


Fig. 6-(a) Fourier Spectra of Microtremors in SPITAK

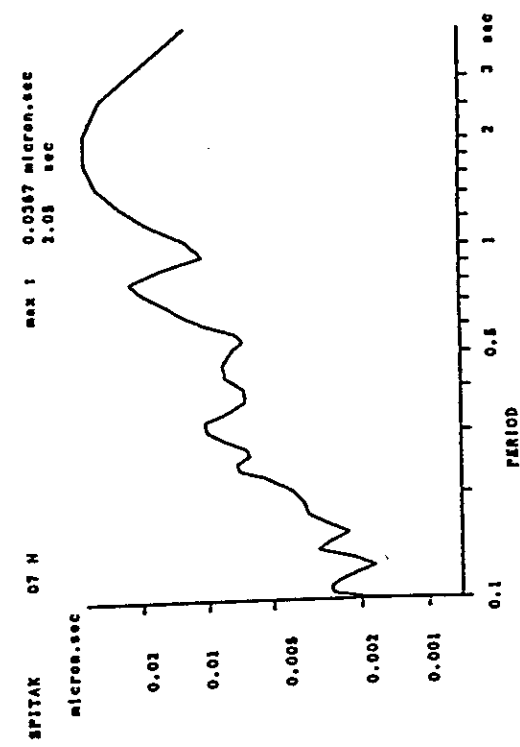
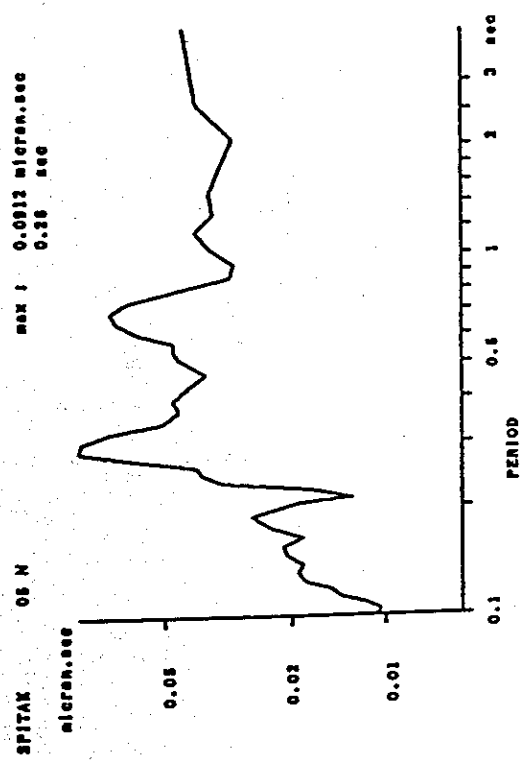
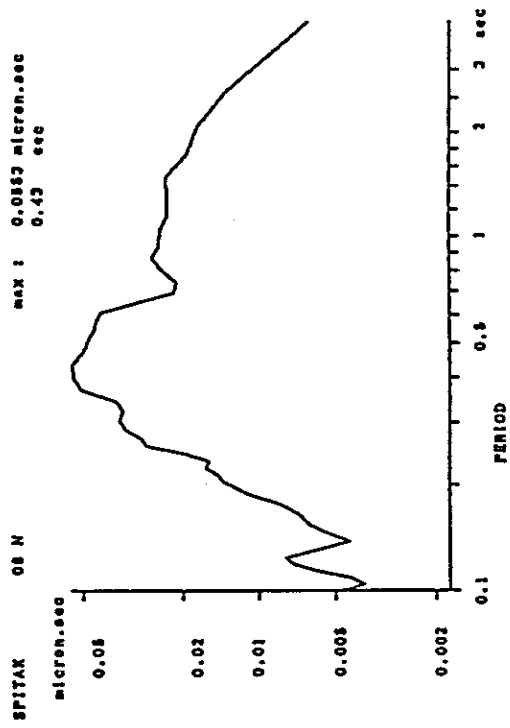
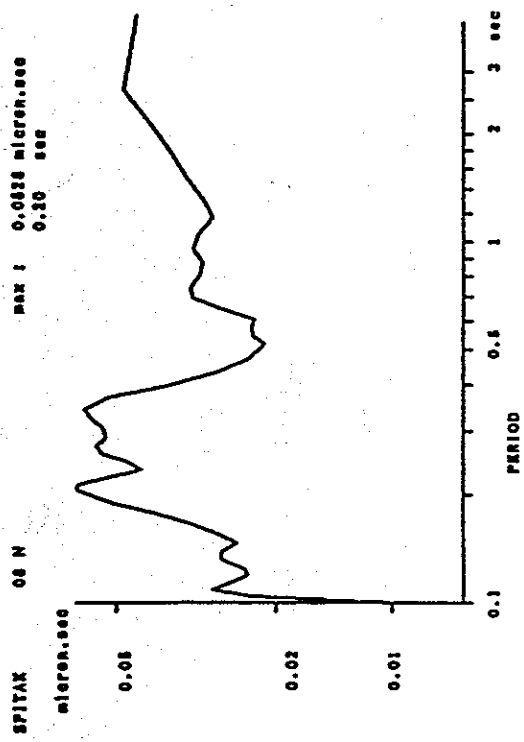


Fig. 6-(b) Fourier Spectra of Microtremors in SPITAK

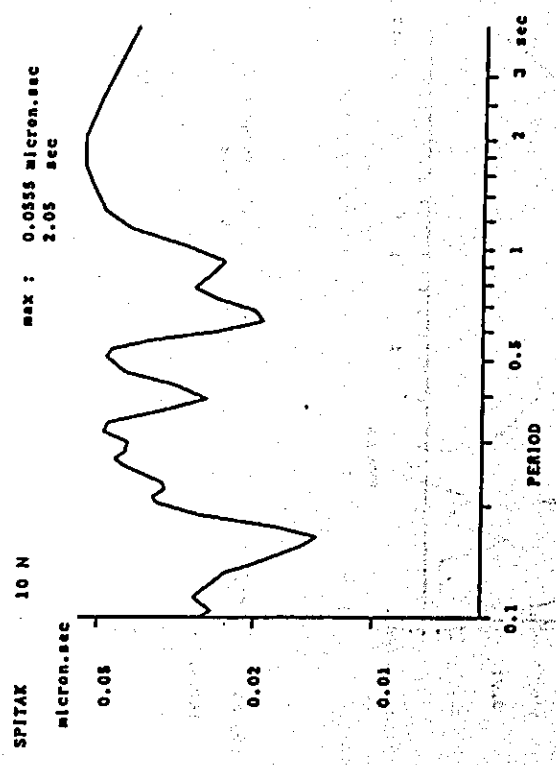
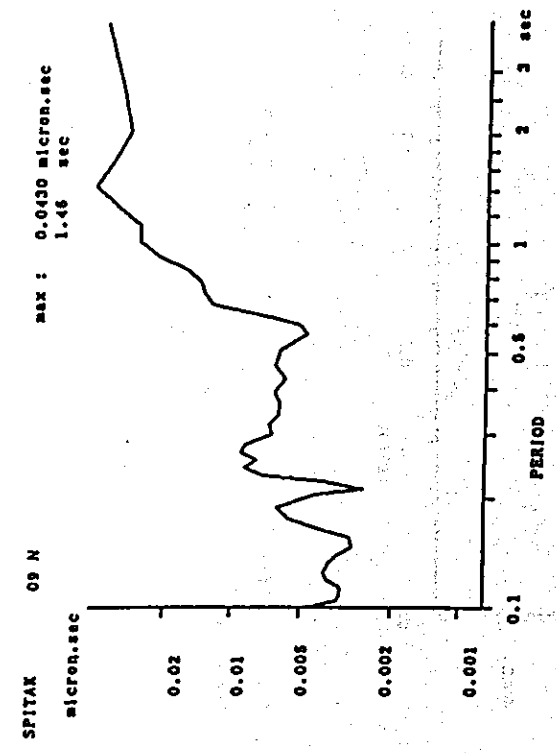


Fig. 6-(c) Fourier Spectra of Microtremors in SPITAX

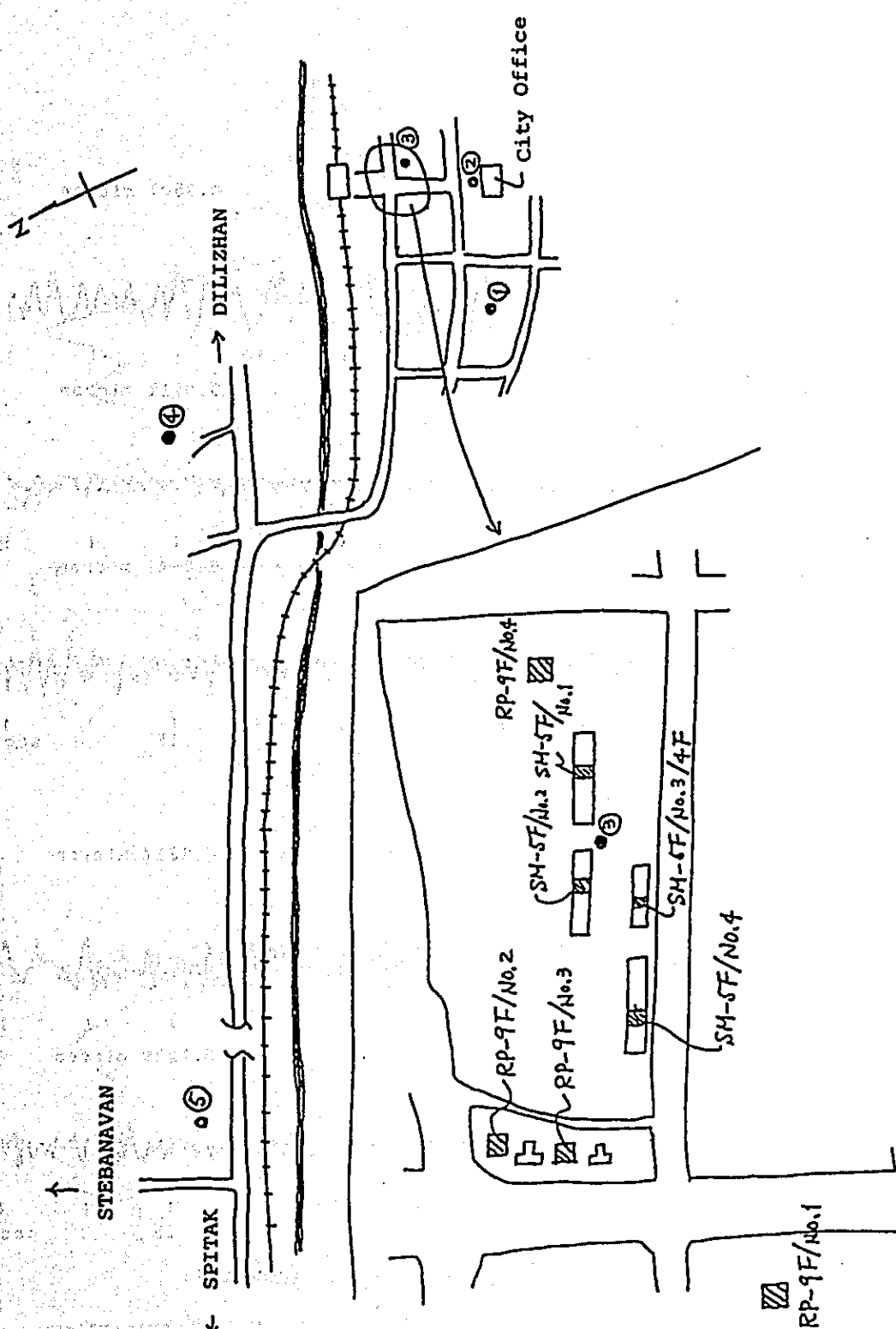
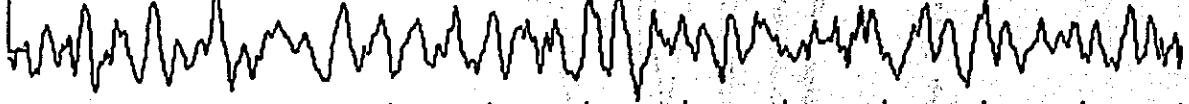


Fig. 7 Measured Points of Microtremors in KIROVAKAN

KIROVAKAN 01 N

0.3507 micron

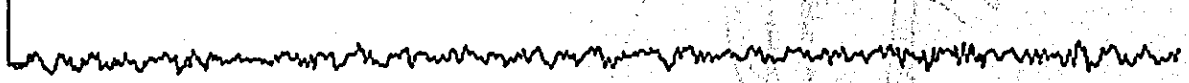
0.4 micron



KIROVAKAN 02 N

0.0911 micron

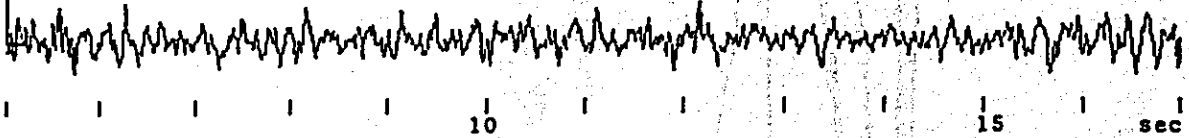
0.4 micron



KIROVAKAN 03 N

0.2242 micron

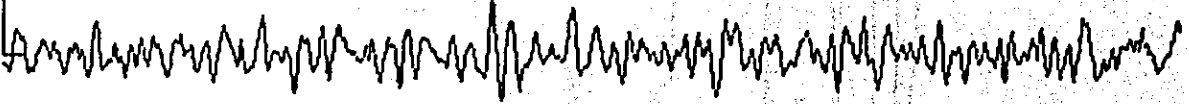
0.4 micron



KIROVAKAN 04 N

0.3324 micron

0.4 micron



KIROVAKAN 05 N

0.1989 micron

0.4 micron

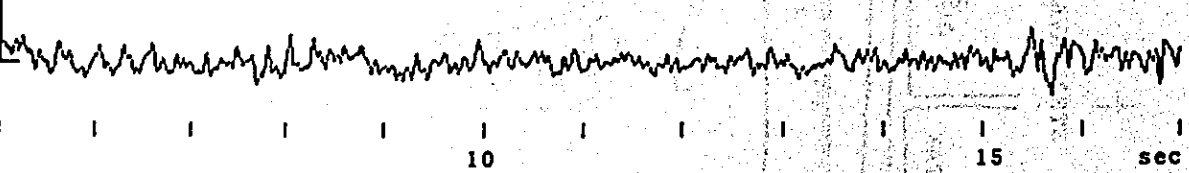


Fig. 8 Wave Forms of Microtremors in KIROVAKAN

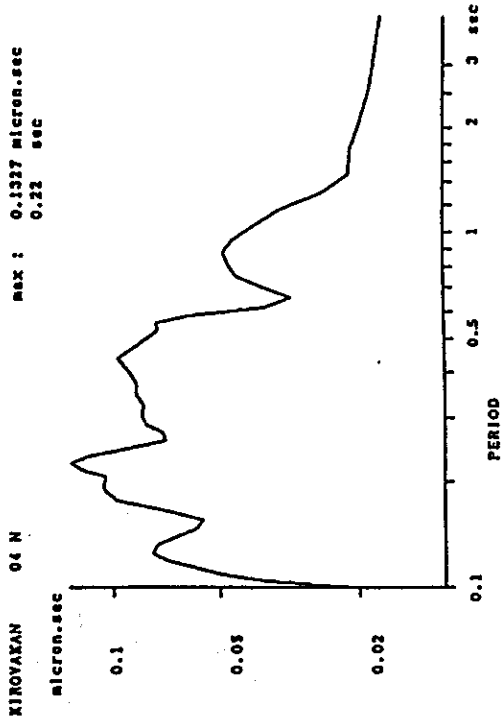
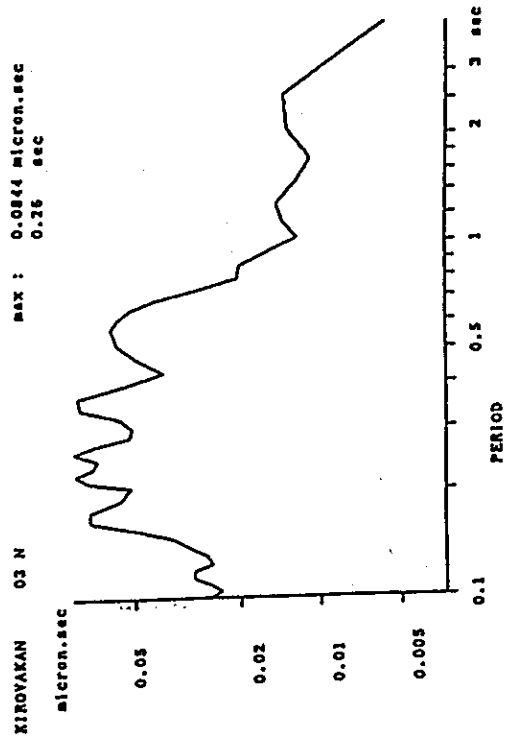
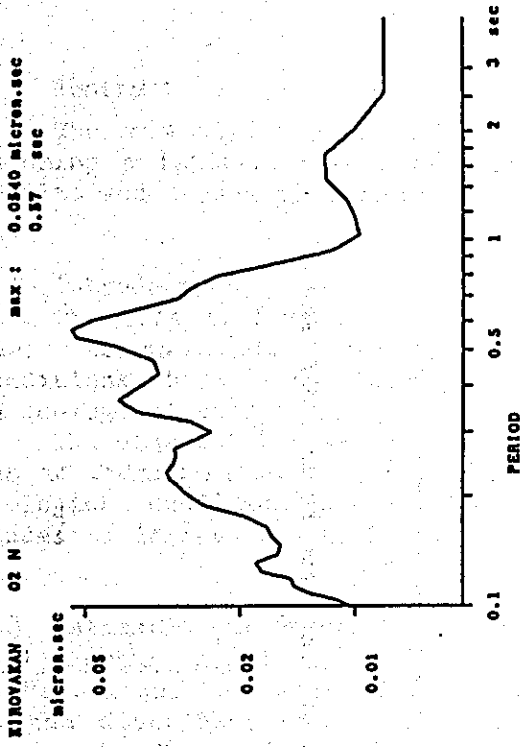
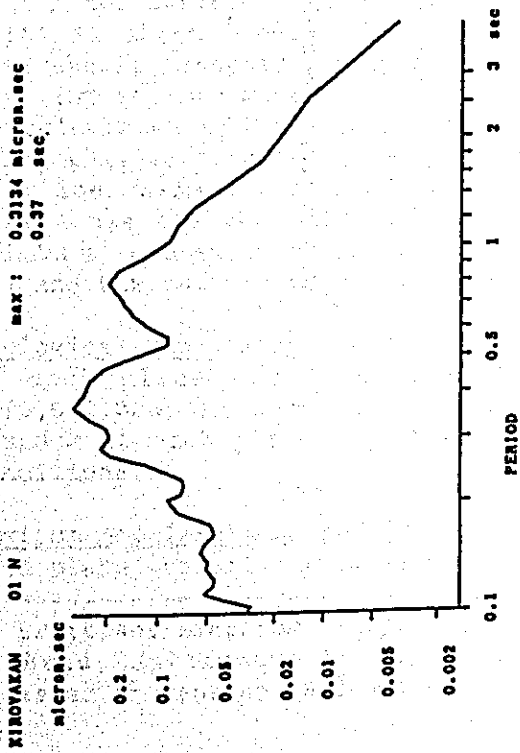


Fig. 9-(a) Fourier Spectra of Microtremors in KIROVAKAN

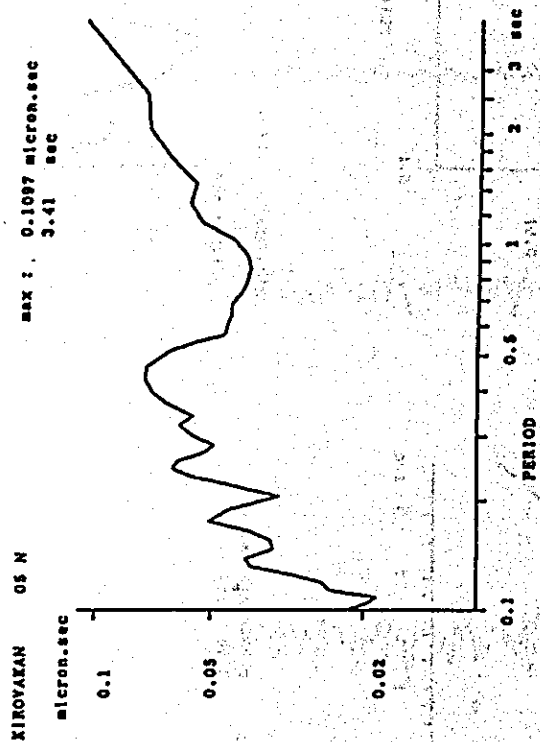


Fig. 9-(b) Fourier Spectra of Microtremors in KIROVAKAN

6. Estimated Intensities of Ground Motions Due to Spitak Earthquake Based on Geological Conditions

6.1 Abstract

The intensities of ground motions due to Spitak Earthquake are estimated by assuming a fault-rupture model and by considering geological conditions. The results and causes of damages due to Spitak Earthquake are discussed.

6.2 Introduction

The lessons learned from past damaging earthquakes have pointed out that there is an evident relation between earthquake damages and geological conditions, because the intensities and characteristics of ground motions depend on geological conditions.

The objects of this paper are to estimate the intensities of ground motions due to Spitak Earthquake by assuming a fault-rupture model and by considering geological conditions and to discuss the relations between their results and the causes of damages due to Spitak Earthquake.

6.3 Estimation of Ground Surface Acceleration

Fault-Rupture Model The location of a fault-rupture model is chosen as shown in Fig. 1 and the parameters of the model are set up as shown in Table 1 based on the distribution of aftershocks shown in Fig. 2 which were measured by Earthquake Research Institute, Armenia Academy of Science and based on the direction and displacement of fault slips discovered in the hill areas on the west of Spitak.

The Fig. 2-(a) is shown the distribution of aftershocks which were measured within the duration between December 7, 1988 and January 15, 1989, and the Fig. 2-(b) is shown because the shape of fault corresponds to the distribution of aftershocks measured within 24 hours after a mainshock.

The seismic moment of the earthquake is the value of 2.5×10^{26} dyne cm which is calculated by the parameters of $L=35\text{km}$, $W=12\text{km}$ and $D=1.5\text{m}$ (mean value) and using this seismic moment, it can be introduced to the magnitude of $M=6.8$ (Table 1). The maximum vertical and horizontal components of the fault slips in the hill areas are the value of 2.0m and 1.8m, respectively and the parameter of $D=1.5\text{m}$ is chosen as the mean value. The dip angle of 60 is assumed by Fig. 2-(c) and the rupture velocity is assumed by experience.

Geological Conditions and Amplification Factors The surface-soil conditions at each place are incorporated on the basis of Armenia geological map (1/6,000,000) as shown in Fig. 3. The amplification factors to the seismic bedrock at each place are shown in Table 2 considering the surface geological conditions.

Maximum Accelerations and Seismic Intensities The maximum accelerations at each place are calculated as the product of those of the incident waves from

-
- *1 Professor Emeritus, Tokyo Institute of Technology
 - *2 Head, Earthquake Engineering Laboratory, National Research center for Disaster Prevention, Science and Technology Agency

the seismic bedrock and amplification factors.¹⁾ The seismic intensities (MSK) are evaluated on the Maximum accelerations which are reduced to about 80% levels of the calculated ones. The reduction factor depends on the experimental relation between maximum accelerations and seismic intensities in Japan.¹⁾ The results are shown in Table 3.

The maximum acceleration level of Spitak 2 in Table 3 is expressed as more than 600gal, as the past results show good agreement in the range of maximum accelerations less than 600gal or so, in case the calculation is carried out in the elastic manner adopted here.¹⁾ The maximum acceleration level of Gukasyan is expressed as more than 228gal, as the geological condition is assumed as hard rock because of the insufficient information.

Discussions

a) The maximum acceleration levels of Gukasyan and Yerevan agree with those of available accelerograms recorded in Gukasyan and Yerevan which are about 200gal (Fig. 4) and 60gal, respectively.

b) The seismic intensities are 10 in Spitak, 9-10 in Leninakan, 8-9 in Kirovakan, 6 in Yerevan in terms of MSK scale and agree with the estimated ones in Armenia.

c) The results are supposed to explain that the intensity of ground motions in Kirovakan more close to the epicenter is lower than that in Leninakan far from the epicenter, although the final judgment requires the exact seismic source mechanism and geological conditions.

6.4 Comments on the Seismic Zoning Map for the Seismic Design

The seismic zoning map for the seismic design is used generally in Armenia. But, the method of seismic zoning map, which is adopted in Soviet, is based upon the method of seismic macro zoning map in Japan. Therefore, the method in Soviet does not consider the method of the micro zoning map, namely based upon the dynamic properties of ground. It is seemed that the method of macro zoning map is mainly based upon the statistical result of the occurrence of historical earthquakes, and is not considered the Seismotectonics, which is strongly insisted by the Soviet Science Academy in former times. This Armenia region is located the very active seismic zone, where the Anatoria fault is closed to the west side of Armenia and the the Zakros seismic belt is connected to the south-eastern direction of the Armenia through the Azerbaizian. The present zoning map of Armenia is difficult to understand the face of the geological structures. We hope that the seismic zoning map will be corrected based upon the results of the distribution of the seismic intensities of each city at this earthquake and the seismotectonics of these area.

6.5 Reference

1) S. MIDORIKAWA and H. KOBAYASHI; "Isoseismic Map in Near-Field with regard to Fault Rupture and Site Geological Conditions" Proceedings of 7th World Conference on Earthquake Engineering, Istanbul, Turkey, Sept., 1980.

Table 1 Parameters of Fault-Rupture Model

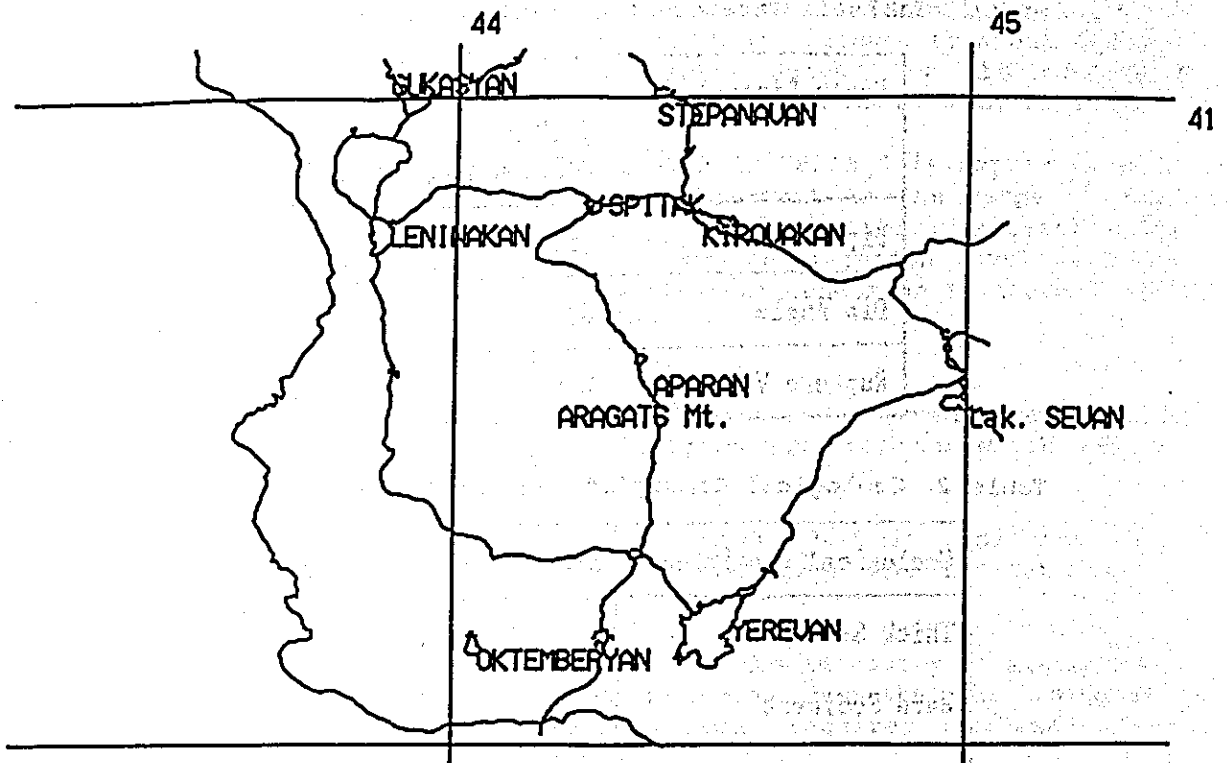
Fault Dimension	L=35 km W=12 km D=1.5 m (mean value)
Dip Direction	N60°W
Dip Angle	60°
Rupture Velocity	2.5 km/sec

Table 2 Geological Conditions and Amplification Factors

Geological conditions	Amplification Factors
Thick Sediment	4.5
Hard Sediment	3.5
Tertiary Period	2.5
Paleogene Period	2.0

Table 3 Maximum Acceleration and Seismic Intensity at Each Place

Place Name	Maximum Acceleration	Seismic Intensity (MSK)	Remarks
SPITAK 2	More than 600 gal	10	Sediment(Deposit)
LENINAKAN 1	530 gal	10	Northern Area
SPITAK 1	520 gal	10	Hard rock
LENINAKAN 2	470 gal	9	Southern Area
STEPANAVAN	460 gal	9	
APARAN	370 gal	9	
KIROVAKAN 2	360 gal	9	Sediment(Deposit)
KIROVAKAN 1	250 gal	8	Central Area
GUKASYAN	More than 228 gal	8	Unidentified Geology
YEREVAN	65 gal	6	



SPITAK USSR EQ Dec. 7 1988

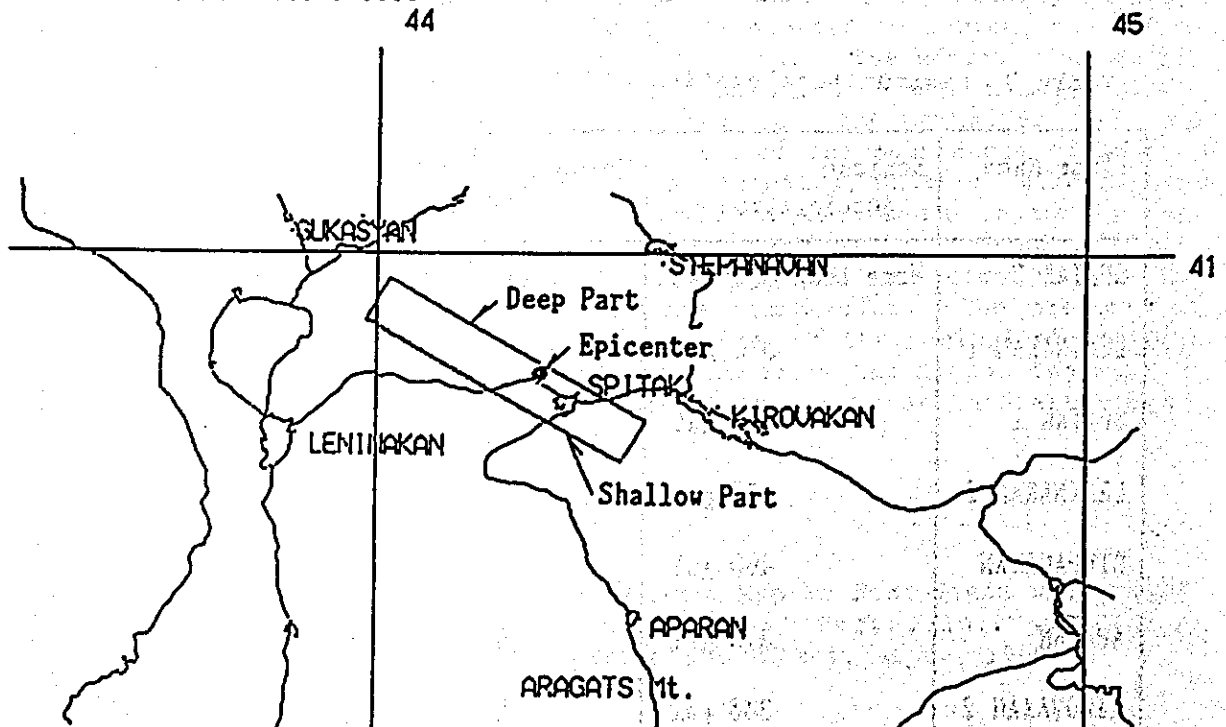


Fig. 1 Location of Fault-Rupture Model

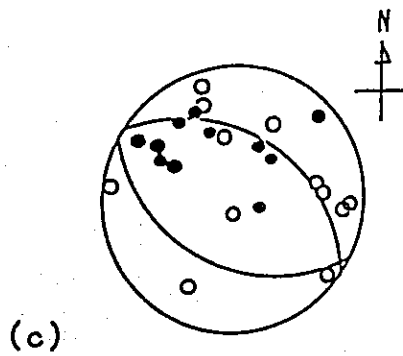
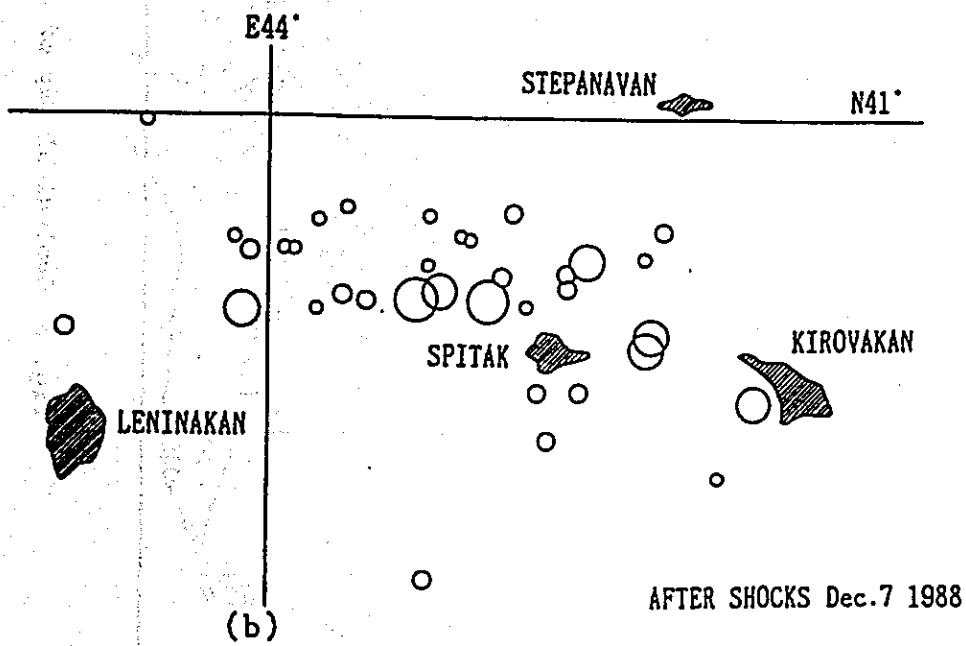
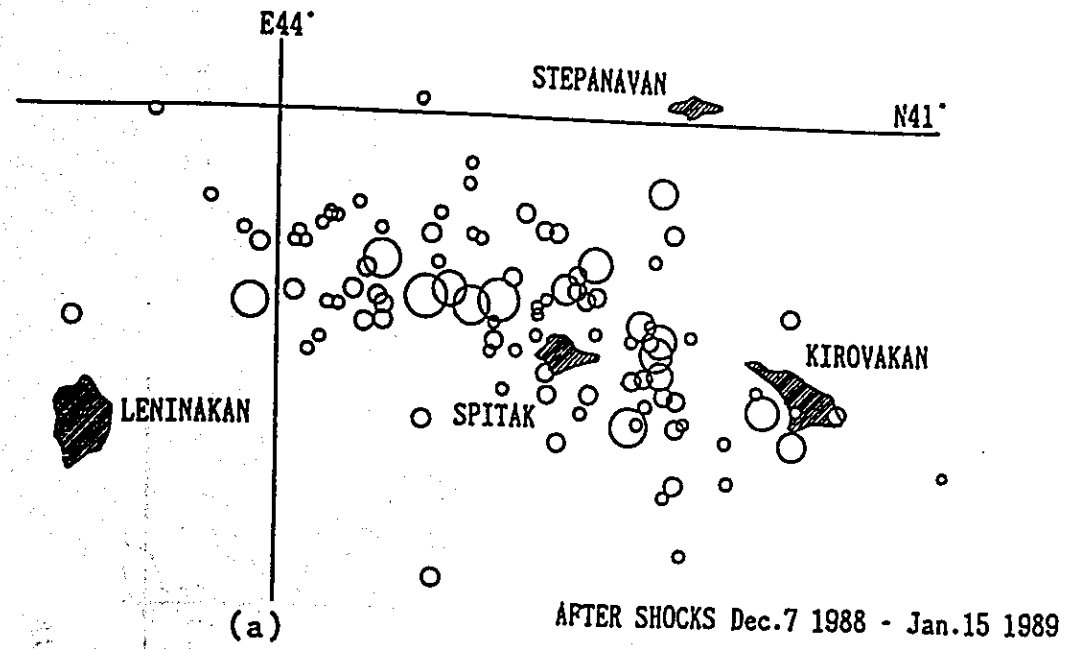


Fig. 2 Distribution of After Shocks

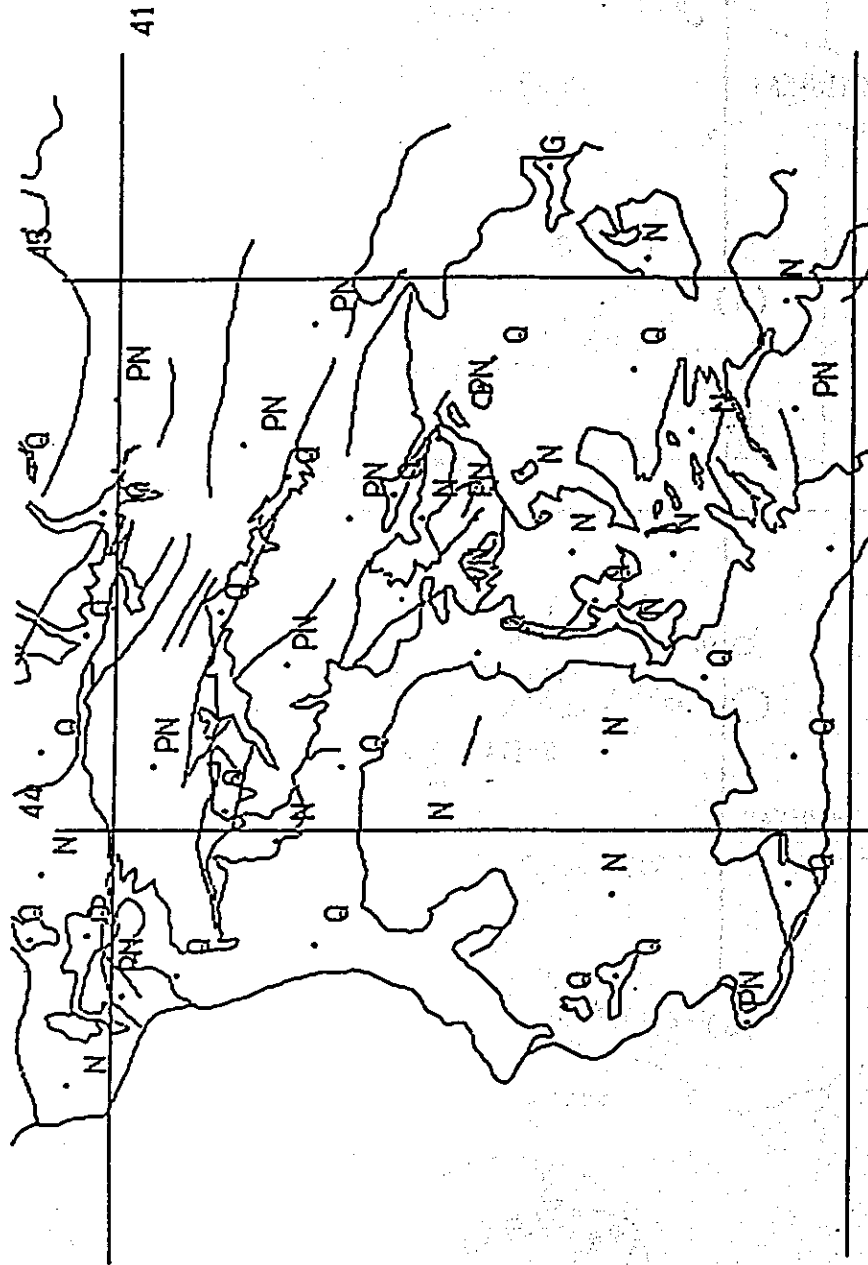


Fig. 3 Geological Map of ARMENIA

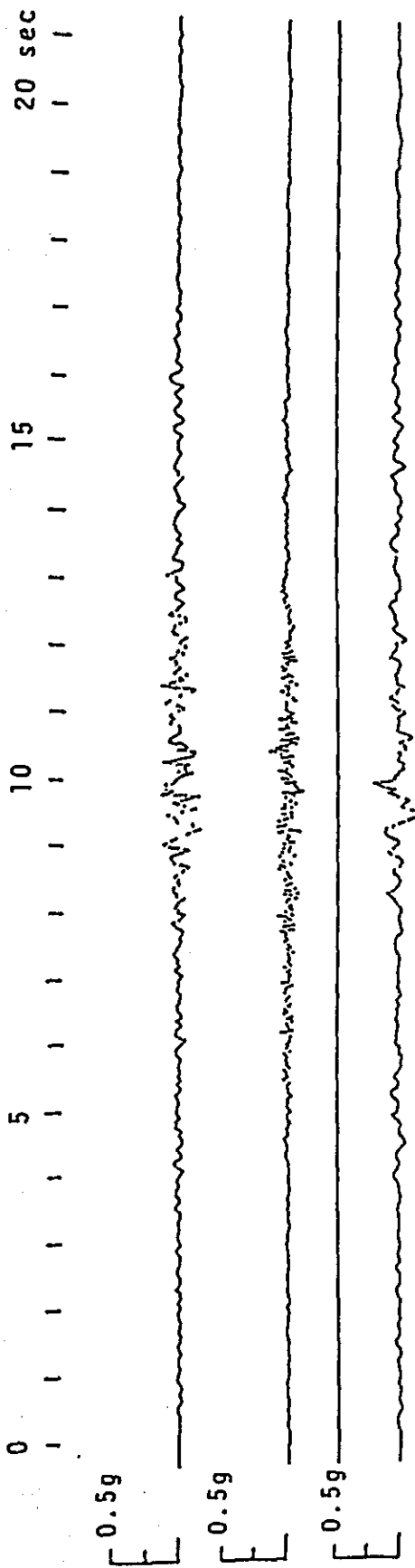


Fig. 4 Strong Motion Accelerogram (GUKASYAN)

JICA